GEOMETRIC SINGULAR PERTURBATION ANALYSIS OF THE YAMADA MODEL†

A. HUBER* AND P. SZMOLYAN**

Abstract. The Yamada model for lasers with saturable absorber is known to display interesting dynamics on widely different time scales. Methods from geometric singular perturbation theory are used to analyze the dynamics. On the slow scale solutions drift along a slow manifold which is attracting on one side of a non-hyperbolic line and repelling at the other side. On the fast scale solutions jump from the repelling part of the slow manifold back to the attracting part. This mechanism generates periodic and homoclinic orbits of relaxation type. A detailed analysis of the complicated behaviour of the homoclinic orbits in the singular limit is given. The recently developed blow-up method for systems of singularly perturbed ordinary differential equations is used to analyze the dynamics near the non-hyperbolic line where an essential part of the dynamics takes place. In the blown-up system a singular homoclinic orbit interacting with a transcritical bifurcation of equilibria is identified. A return map along the singular homoclinic orbit is studied to prove that the homoclinic orbit persists along a smooth curve in parameter space which is shown to be exponentially close to the transcritical bifurcation curve.

Key words. laser dynamics, slow-fast dynamics, blow-up method, homoclinic orbits

AMS subject classifications. 34C26, 34C37, 34E15, 37G05, 37N20

1. Introduction. Lasers with saturable absorber are known for their sustained laser oscillations, consisting of pulse trains of extremely short hight intensity laser output of high frequency. This behaviour, also called passive Q-switching or self pulsing, was observed in many different kinds of laser systems. Experimental and numerical studies show their existence for CO_2 laser [1, 24]. They where also observed for microchip solid state lasers [10, 21, 29]. We are mainly interested in semiconductor lasers which show high repetition rates from hundreds of megahertz to tenth of gigahertz [12, 14, 28]. They are interesting for telecommunication and for optical data storage using compact disc (CD) and digital versatile disc (DVD) systems. Other applications are the reduction of optical feedback noise in semiconductor injection lasers and for optical timing extraction by injection locking of self pulsing optical oscillators. For further information see [8, 12, 13, 14].

In lasers driven by a constant pumping power, self-pulsation is a result of the nonlinear interaction of the slowly responding amplifying and absorbing media and the fast response of the electric field. The basic mechanism generating these oscillations can be described roughly as follows. When the laser is turned on, the amplifying medium, the gain, is excited through some pumping process. However the absorber absorbs the free photons in the laser, therefore the electric field intensity stays low and the saturation of the gain continues. When the absorbing medium saturates, the ordinary laser process starts with a strongly excited gain which leads to a high intensity of the electric field and therefore a greatly enhanced output power. During this process the gain and the absorber turn to ground state again and the process starts anew.

In the past decade dynamical system approaches to the analysis of lasers have been quite successful [20, 27]. A characteristic feature of lasers with obvious practical importance is that by changing the material or - even more simple - by solely changing the pump power, the qualitative behaviour of the laser beam can change dramatically [14], i.e. a large variety of local and global bifurcations has been found. The occurrence of vastly different time scales makes numerical simulations of lasers challenging and time consuming. On the other hand it allows to use perturbation methods to get simple approximate equations which are easier to analyze [7, 8, 10].

†A short summary of the results presented in this paper have been submitted to the proceedings of the EQUADIFF 2003 conference.

*Institut für Mathematik I, Freie Universität Berlin, Arnimalle 2-6, D-14195 Berlin, Germany.

**Institut für Angewandte und Numerische Mathematik, Technische Universität Wien, Wiedner Hauptstraße 8-10, A-1040 Wien, Austria. This research was supported by the Austrian Science Foundation under grant Y 42-MAT.

For an overview and comparison of different rate equation models for laser diodes with saturable absorber see [2]. Solid state microchip lasers, semiconductor lasers and CO_2 lasers are often described by one system of rate equations, but with different ranges of parameters [7, 8, 9, 10, 13, 14].

We consider the Yamada model [14], for lasers with a saturable absorber,

$$\begin{aligned} \dot{I} &= (G - Q - 1)I \\ \dot{G} &= \varepsilon(A - G - GI) \\ \dot{Q} &= \varepsilon(B - Q - aQI), \end{aligned} \tag{1.1}$$

which is derived from the model proposed in [28]. The system of rate equations (1.1) is equivalent to the model considered by Erneux and coworkers [7, 9], if we rescale the variables and parameters and set $\bar{\gamma} = \gamma$ (in [9]).

In [7, 9] an asymptotic analysis of the rate equations using matched asymptotic expansions is given and bifurcation diagrams showing the dependence of the qualitative behaviour on parameters are provided. The fast pulsations of the laser intensity correspond to periodic orbits of the rate equations. Erneux gives a formal asymptotic description of the periodic orbits and indicates that these periodic orbits are generated in a bifurcation from a homoclinic orbit [7]. Complementing these results we give a detailed analysis of this basic homoclinic orbit and its rather complicated singular limit. The methods used in our analysis could be also used to study the existence of periodic orbits and their bifurcation from the homoclinic orbit.

System (1.1) is written in scaled dimensionless variables, where I denotes the laser intensity, G the population density in the amplifying medium, and Q the population density in the absorbing medium. Because of the physical restrictions of the model we consider the region $I \geq 0$, $G \geq 0$ and $Q \geq 0$, only. The parameter A is proportional to the pump current, the parameters a and B specify the the relative absorption rates and remain fixed in a typical experiment. The parameter ε is due to the different time scales of the field intensity and the amplifying and absorbing media. Since ε is very small, i.e. the typical order of magnitude is $10^{-3} - 10^{-4}$, system (1.1) is singularly perturbed.

The experimentally observed high frequency pulses correspond to periodic orbits of system (1.1). In [14] an interesting bifurcation analysis with respect to the parameters a,B,A, ε has been carried out by combining analytical and numerical methods. For ε small only a few basic bifurcations occur. The most interesting situation occurs by varying A, ε for constant parameters $a > 1, B > \frac{1}{a-1}$. Analytical calculations show the occurrence of saddle-node, transcritical, and Hopf bifurcations for $\varepsilon > 0$ along curves $A = A_{SN}(\varepsilon)$, $A = A_T(\varepsilon) = B + 1$, and $A = A_{Hopf}(\varepsilon)$, $\varepsilon \in [0, \varepsilon_0]$. More details are given in Sect. 2, e.g. see Figure 2.3.

The numerical calculations in [14] indicate that a homoclinic orbit exists along a curve $A = A_{Hom}(\varepsilon)$. The curves $A = A_{Hom}(\varepsilon)$ and $A = A_T(\varepsilon)$ seem to be extremely close and seem to meet at $(A, \varepsilon) = (B, 0)$. The singular limit $\varepsilon \to 0$ was not considered in detail there. It is one goal of this work to fill in some analytical details on the dynamics of system (1.1) for small values of ε.

In this work we give a detailed geometric analysis of the complicated global dynamics and local bifurcations near the point $(A, \varepsilon) = (B, 0)$. We show analytically that the curve of homoclinic orbits exists and that the two curves $A = A_{Hom}(\varepsilon)$ and $A = A_T(\varepsilon)$ indeed intersect for $\varepsilon = 0$. Further we show that the curves are exponentially close for $\varepsilon \to 0$, that is $|A_{Hom}(\varepsilon) - A_T(\varepsilon)| = O(e^{-c/\varepsilon})$.

For the proof we transform to $J = \varepsilon I$ because this is the natural scale for the intensity I. We get a singularly perturbed differential equation where the critical manifold is given by $S_0 = \{J = 0\}$. The line $L := \{J = 0, G - Q - 1 = 0\}$ separates the critical manifold in an attracting part $\{J = 0, G - Q - 1 < 0\}$ and a repelling part $\{J = 0, G - Q - 1 > 0\}$. Outside of a neighbourhood of the line L geometric singular perturbation theory [16, 18] is directly applicable. On L the crucial condition of normal hyperbolicity is violated. However the

essential dynamics of the homoclinic bifurcation takes place close to the line L. Therefore we use a blow-up transformation of the non-hyperbolic line L to describe the dynamics there. In the blown-up problem we find a regular transcritical bifurcation at $\varepsilon = 0$ and a singular homoclinic orbit at $\varepsilon = 0$. This can be used to prove (i) the existence of the homoclinic orbit, and (ii) the exponential closeness of the curves $A = A_L(\varepsilon)$ and $A = A_T(\varepsilon)$ for small values of ε.

In the past few years the blow-up method has been applied successfully to a number of interesting singular perturbation problems involving non-hyperbolic points [4, 5, 6, 22, 23]. The problems treated in these works were planar. This work shows that also for higher dimensional problems the blow-up method is an effective tool to analyze singularly perturbed equations near non-hyperbolic lines.

2. Slow fast structure and bifurcations. The plane $I = 0$ is invariant under the flow of system (1.1), and for $I = O(\varepsilon)$ the dynamics is slow and solutions drift toward $(G, Q) = (A, B)$. Away from the plane $I = 0$ pulse like jumps occur during which the variables G and Q decrease monotonously. Along these pulses the variable I has maximum values of order $O(\frac{1}{\varepsilon})$. To capture these pulses we perform the rescaling $I = \frac{J}{\varepsilon}$. In these variables system (1.1) has the form

$$\begin{aligned} J' &= (G - Q - 1)J \\ G' &= -GJ + \varepsilon(A - G) \\ Q' &= -aQJ + \varepsilon(B - Q), \end{aligned} \tag{2.1}$$

which will be the starting point of our analysis.

Setting $\varepsilon = 0$ in (2.1) we obtain the layer problem

$$\begin{aligned} J' &= (G - Q - 1)J \\ G' &= -GJ \\ Q' &= -aQJ, \end{aligned} \tag{2.2}$$

which is the limiting problem of the fast dynamics. The equilibria of the layer problem are given by the 2−dimensional critical manifold $S_0 := \{J = 0\}$. The set of stable equilibria S_0^s of S_0, with $G - Q - 1 < 0$, and the set of unstable equilibria S_0^u, with $G - Q - 1 > 0$, are separated by the line L of non-hyperbolic equilibria.

Lemma 1. *The orbit of the layer problem passing through $(J_{out}, G_{out}, Q_{out})$ lies on the invariant curve*

$$\begin{aligned} Q(G) &= \frac{Q_{out}}{G_{out}^a} G^a \\ J(G) &= ln(G) + \frac{1}{a}\frac{Q_{out}}{G_{out}^a} G^a - G + J_{out} - ln(G_{out}) - \frac{1}{a} Q_{out} + G_{out}, \end{aligned} \tag{2.3}$$

(see Fig. 2.1).

Proof: System (2.2) has the conserved quantities

$$\begin{aligned} H_1(G, Q, J) &= \frac{Q}{G^a} \\ H_2(G, Q, J) &= J - \frac{1}{a} Q + G - ln(G). \end{aligned} \tag{2.4}$$

Solving the equations $H_1(G, Q, J) = H_1(J_{out}, G_{out}, Q_{out})$,
$H_2(G, Q, J) = H_2(J_{out}, G_{out}, Q_{out})$ for Q, J provides the assertions. □

Thus, heteroclinic orbits of the layer problem with $J(t)|_{t=\pm\infty} = 0$ can be used to jump from S_0^u to S_0^s. Three such heteroclinic orbits are shown in Fig. 2.2 in green colour. Points P on the line L with $Q_{out} > \frac{1}{a-1}$ are also connected to points in S_0^s by a heteroclinic orbit,

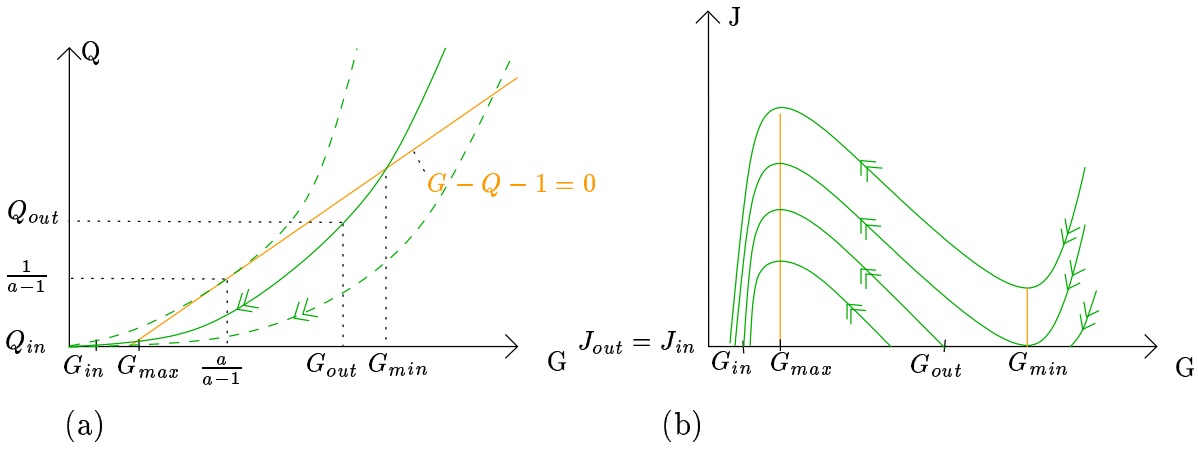

FIG. 2.1. *Dynamics of the layer problem, (a) Q versus G and (b) J versus G along an orbit* $\frac{Q}{G^a}=\frac{Q_{out}}{G^a_{out}}$

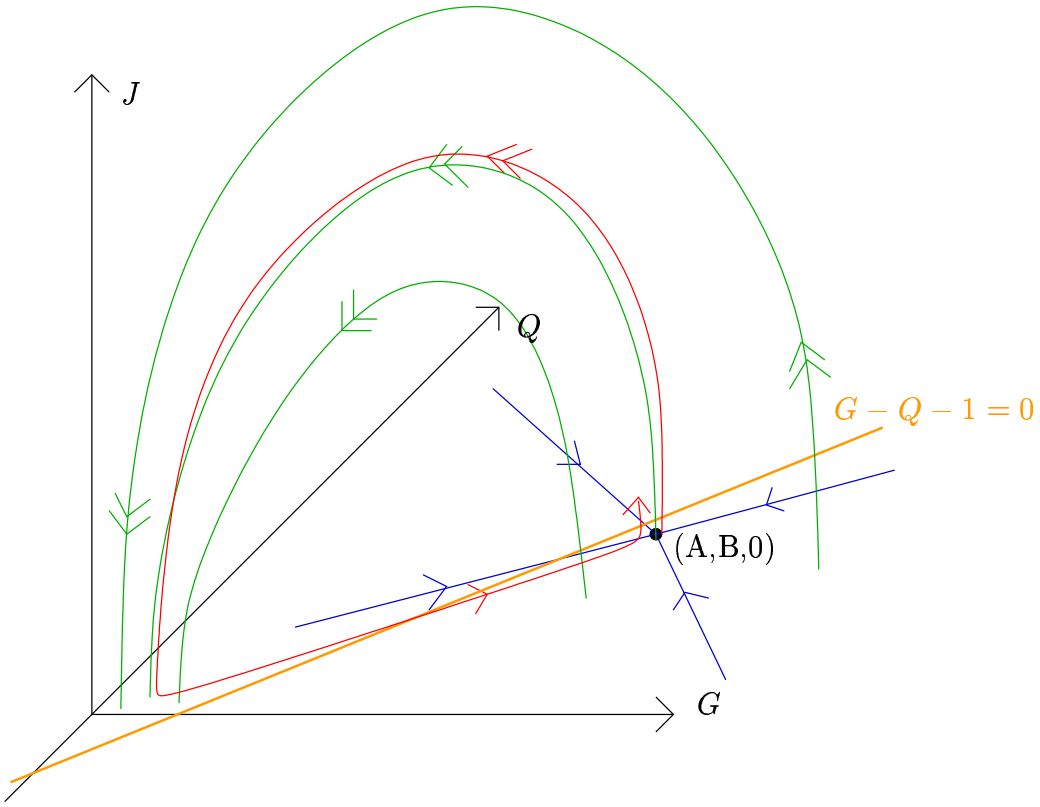

FIG. 2.2. *The basic dynamics of the Yamada model*

however, these orbits are tangent to $J=0$ and non-hyperbolic near P. For $Q_{out}\geq c>\frac{1}{a-1}$, $G_{out}-Q_{out}-1\geq 0$ the endpoints of these heteroclinic orbits satisfy $G_{in}-Q_{in}-1\leq\delta(c)<0$. For $J\geq\delta$, $\delta>0$ small, the solutions of the original equations are regular perturbations of the solutions of the layer problem.

The reduced system for the laser equations (2.1), which describes the slow flow on S_0

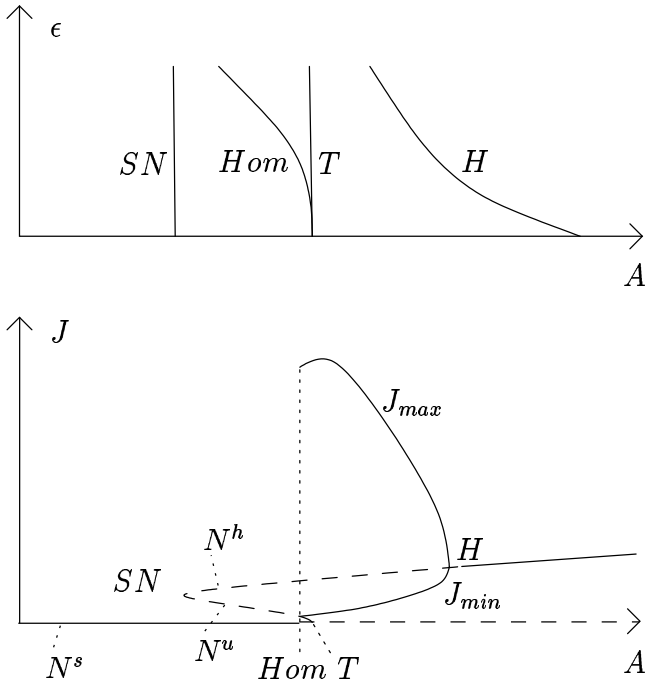

FIG. 2.3. *The bifurcations of the Yamada model*

on the slow time scale $\tau = \varepsilon t$, is

$$\begin{aligned} \dot{G} &= A - G \\ \dot{Q} &= B - Q. \end{aligned} \tag{2.5}$$

In this linear system, $(G, Q) = (A, B)$ is the globally stable equilibrium (see Fig. 2.2, blue lines).

We define the stable normally hyperbolic part of S_0, S_H^s, by $G - Q - 1 \leq \delta_2$ and the unstable hyperbolic part of S_0, S_H^u, by $\delta_1 \leq G - Q - 1$ for some fixed small $\delta_1 > 0$, $\delta_2 < 0$.

In general normally hyperbolic critical manifolds perturb to slow manifolds for ε small [16, 18]. Since $J = 0$ is invariant for system (2.1) the slow manifold S_ε is globally given by $J = 0$ and the flow on S_ε is given by (2.5), even for $\varepsilon > 0$.

Solutions near S_H^s are attracted to the slow manifold S_ε with an exponential rate of order $O(e^{-at})$ with $a > 0$ transversally to S_ε while following the flow in S_ε. Analogously solutions near S_H^u will be repelled with an exponential rate of order $O(e^{bt})$ with $b > 0$ transversally from S_H^u while following the flow in S_ε.

By collecting these properties we obtain the following qualitative description of the dynamics of system (2.1). An orbit starting slightly above S_H^u follows closely an orbit of the layer problem, i.e. the orbit jumps to the attracting slow manifold. The slow drift along the slow manifold occurs. The orbit is exponentially attracted onto S_0 to the left of the hon-hyperbolic line. When the orbit crosses the plane $G - Q - 1 = 0$ J is exponentially small, thus the orbit follows the slow dynamics in S_H^u for a while before it is repelled again. Then this process may repeat. A typical orbit is shown in Fig. 2.2 in red. This basic reinjection mechanism allows for oscillatory, periodic and homoclinic behaviour.

We now briefly summarize parts of the bifurcation analysis of [14]. Bifurcations occur by variation of the parameters A, B, a and ε. We take $a > 1$, $B > \frac{1}{a-1}$ constant and describe the bifurcations which occur by varying A, ε for small ε.

The equilibrium $N^s := (A, B, 0)$ exists for all values of A and ε. It is attracting for $A - B - 1 < 0$ and repelling in J direction for $A - B - 1 > 0$. For $\varepsilon > 0$ up to two equilibria,

N^u and N^h, with $J > 0$ exist in the plane $G - Q - 1 = 0$ which bifurcate from the non-hyperbolic line for $\varepsilon \to 0$. For $A = A_{SN}(\varepsilon)$ the equilibria N^u and N^h of saddle type appear in a saddle node bifurcation. For $A = A_{Hom}(\varepsilon)$ numerical calculations indicate that an orbit homoclinic to the equilibrium N^u exists. For $A > A_{Hom}(\varepsilon)$ numerics indicate the existence of a family of periodic orbits which begins at the homoclinic orbit at $A = A_{Hom}(\varepsilon)$. At $A = A_T(\varepsilon) = B + 1$ the equilibrium N^u with $J > 0$ coalesces with the equilibrium N^s in $J = 0$ in a transcritical bifurcation and the equilibrium $N^s = (A, B, 0)$ loses stability in the J direction. The periodic orbit becomes smaller and then disappears in a Hopf bifurcation at $A = A_H(\varepsilon)$, where the equilibrium N^h becomes attracting. The bifurcation curves are ordered by $A_{SN}(\varepsilon) < A_{Hom}(\varepsilon) \leq A_T(\varepsilon) < A_H(\varepsilon)$. The situation is illustrated in Figure 2.3. In the lower picture of Fig. 2.3 the J-values of the equilibria with $J > 0$ for the different values of A are shown. The equilibria N^u, N^h satisfy $G - Q - 1 = 0$ whereas the equilibria N^s lies on the line $Q = B$. At the transcritical bifurcation $A = A_T$ the curve of equilibria N^u intersect with the line of equilibria N^s in $J = 0$. The curves J_{min}, J_{max} correspond to the minima and maxima of J along the family of periodic orbits.

3. Main results and the blow-up transformation. We show the following Theorem for the Yamada Equations:

Theorem 1. *For $a > 1$, $B > \frac{1}{a-1}$ there exists a $\varepsilon_0 > 0$ such that*

1. *there exists a C^1-function $A_{Hom}(\varepsilon)$, $\varepsilon \in [0, \varepsilon_0]$, such that for $A = A_{Hom}(\varepsilon)$ an orbit homoclinic to N^u exists,*
2. *the functions $A_T(\varepsilon)$ and $A_{Hom}(\varepsilon)$ are exponentially close, that means, there exists $c > 0$ such that $|A_{Hom}(\varepsilon) - A_T(\varepsilon)| < O(e^{-c/\varepsilon})$ for $\varepsilon \in [0, \varepsilon_0]$.*

The transcritical bifurcation occurs for $(A_T, B, 0)$ on the non-hyperbolic line L and parts of the homoclinic orbit are close to L as well. Therefore, we need a detailed analysis of the dynamics near the non-hyperbolic line. The parameters a, B are kept constant in the following. We make the coordinate transformation

$$\begin{aligned} D &= G - Q - 1 \\ H &= G - 1 \\ \Delta &= A - B - 1, \end{aligned} \tag{3.1}$$

and obtain the equations

$$\begin{aligned} J' &= DJ \\ D' &= ((a-1)H - 1 - aD)J + \varepsilon(\Delta - D) \\ H' &= -(H+1)J + \varepsilon(B + \Delta - H) \\ \varepsilon' &= 0 \\ \Delta' &= 0. \end{aligned} \tag{3.2}$$

We will see that adding the trivial equations is important in the blow-up transformation. In these variables $\{D = 0\}$ describes the non-hyperbolic line. $\{J = 0, D < 0\}$ is now the stable part of the slow manifold S_0^s and $\{J = 0, D > 0\}$ the unstable part S_0^u. The equilibrium $(J, G, Q) = (0, A, B)$ is given by $(J, D, H) = (0, \Delta, B + \Delta)$. The transcritical bifurcation occurs now for $\Delta_T(\varepsilon) = 0$ and we will show that

$$|\Delta_{Hom}(\varepsilon)| = |A_{Hom}(\varepsilon) - B - 1| < O(e^{-c/\varepsilon}).$$

We perform a blow-up transformation of the line $\{D = 0, J = 0, \Delta = 0, \varepsilon = 0\}$ in the extended phase space $(J, D, H, \varepsilon, \Delta)$ to understand the dynamics of system (3.2) in a neighborhood of the non-hyperbolic line. The blow-up transformation

$$\begin{aligned} \psi : \quad & \mathbb{R}^3 \times S_2 \quad \to \mathbb{R}^5 \\ & (\bar{r}, \bar{H}, \bar{\Delta}, \bar{J}, \bar{D}, \bar{\varepsilon}) \to (J, D, H, \varepsilon, \Delta) \end{aligned}$$

is defined by

$$J = \bar{r}^2 \bar{J},\ D = \bar{r}\bar{D},\ H = \bar{H},\ \varepsilon = \bar{r}\bar{\varepsilon},\ \Delta = \bar{r}\bar{\Delta} \tag{3.3}$$

with $(\bar{J}, \bar{D}, \bar{\varepsilon}) \in S_2$. Since ψ is a C^∞ diffeomorphism for $\bar{r} > 0$ it maps orbits to orbits and we get an equivalent system of differential equations for $\bar{r} > 0$. The main reason for this transformation is that in the blown-up system it is possible to desingularize the vector field on $\{\bar{r} = 0\} = \psi^{-1}(0, 0, \mathbb{R}, 0, 0)$, and to use the flow on $\{\bar{r} = 0\}$ in the analysis of the dynamics for $\bar{r}$ small.

To make calculations as easy as possible we introduce directional charts as follows:

1. Chart K_1, which is defined by

$$J = r_1^2 J_1,\ D = -r_1,\ H = H_1,\ \varepsilon = r_1\varepsilon_1,\ \Delta = r_1\Delta_1$$

   on $\mathbb{R}^5$ with $r_1 \geq 0$, $\varepsilon_1 \geq 0$, describing the flow for $\bar{D} < 0$.
2. Chart K_2, which is defined by

$$J = r_2^2 J_2,\ D = r_2 D_2,\ H = H_2,\ \varepsilon = r_2,\ \Delta = r_2\Delta_2$$

   on $\mathbb{R}^5$ with $r_2 \geq 0$, describing the flow for $\bar{\varepsilon} > 0$.
3. Chart K_3, which is defined by

$$J = r_3^2,\ D = r_3 D_3,\ H = H_3,\ \varepsilon = r_3\varepsilon_3,\ \Delta = r_3\Delta_3$$

   on $\mathbb{R}^5$ with $r_3 \geq 0$, $\varepsilon_3 \geq 0$, describing the flow for $\bar{J} > 0$.

The laser equations have five time-dependent variables after the blow-up transformation, hence it is not easy to visualize the blown-up system. The non-hyperbolic line is blown up to the manifold $\mathbb{R}^2 \times S_2$. This is illustrated in Fig. 4.1(b),(d) where ε and Δ are not shown.

In Fig. 4.1(a),(c) the part of the cylinder $H = B$ is shown. In these two figures we see, which chart is used to describe the dynamics in each region. Figure 4.1(a) shows the relevant behaviour for $\Delta < 0$ and Figure 4.1(c) for $\Delta = 0$. The green lines describe the fast fibers of the layer problem, the blue dots the critical manifold, the cylinder $\bar{r} = 0$ is shown yellow. The colour red is used for $\varepsilon > 0$. Near $J = 0$, $H = B$ is attracting, $H = B$ is invariant on $\bar{r} = 0$.

The meaning of the equilibria in the blown-up system compared to the original system (2.1) is the following: S_0^s and S_0^u are the stable and the unstable part of the critical manifold, N^s and N^u are the equilibria of the bifurcation analysis for different values of ε, which intersect in the transcritical bifurcation at $\Delta = 0$. The curves of equilibria, the entrance and exit points to the cylinder, l^i and l^0, exist only for $\bar{r} = 0$, and are therefore not visible in the original system (2.1). They intersect for $B = \frac{1}{a-1}$, which is a more degenerate bifurcation point (see [14]).

4. Proof of Theorem 1. The proof is carried out in several steps in the following subsections of the paper and in the appendix, for a summary of the different steps see subsection 4.7 and in particular Figure 4.14. Here we start with a short description of the strategy of the proof of Theorem 1.

We will work exclusively with the blown-up system. The result for the original system follows by the blow-down transformation. We will show that the blown-up system has a homoclinic orbit for $\Delta = \Delta_{Hom}(\varepsilon)$. Each of these homoclinic orbits $\gamma(\varepsilon, \Delta_{Hom})$ starts (for $t \to -\infty$) at an equilibrium in the manifold of equilibria N^u in $H = B$ (see Fig.4.1 (a)). Then the orbit $\gamma(\varepsilon, \Delta_{Hom})$ follows the flow near the cylinder $\bar{r} = 0$ to the exit line (near $H = B$) of equilibria l^o where it jumps away from the cylinder to the stable part of the slow manifold S_ε^s with a positive distance to the singular line. During this jump it follows the solutions of the layer problem (dashed line). Then $\gamma(\varepsilon, \Delta_{Hom})$ is attracted to S_ε^s exponentially close and near to $H = B$. After that the orbit follows the flow near the cylinder again until it ends (for $t \to \infty$) in the equilibrium in N^u again.

To show this we will follow all orbits $\gamma(\varepsilon, \Delta)$ of the unstable manifold of N^u with ε, Δ small. For $\Delta = 0, \bar{r} = 0$ the equilibria N^s and N^u coalesce in a point o. For $\varepsilon = 0$ there exists a singular homoclinic orbit for $\Delta_{Hom} = 0$, which starts in o (see Fig. 4.1(c)). The singular orbit $\gamma(0,0)$ consists of 4 different parts:

- the orbit on the cylinder connecting o to the exit point p^o,
- the orbit of the layer problem which connects p^o to an equilibrium in the critical manifold S_0,
- the solution in the critical manifold to the equilibrium p on the cylinder and
- the orbit on the cylinder from p to o.

For $\varepsilon \geq 0, \Delta \geq 0$ the 2-parameter family of orbits $\gamma(\varepsilon, \Delta)$ is a 3-dimensional manifold close to the singular orbit $\gamma(0,0)$. The orbits of this manifold follow $\gamma(0,0)$ to the stable part of the slow manifold S^s_ε and are attracted exponentially close to $J = 0$. Afterwards they follow $\gamma(0,0)$ close to the cylinder.

We will prove that $\gamma(\varepsilon, \Delta)$ intersects M^s, the stable manifold of N^u for small ε. This allows to prove the existence of the homoclinic orbit for $\Delta = \Delta_{Hom}(\varepsilon)$, where $\Delta_{Hom}(\varepsilon)$ has the properties described in Theorem 1. For $\Delta < \Delta_{Hom}$ the orbits $\gamma(\varepsilon, \Delta)$ converge to the stable equilibria in N^s and for $\Delta > \Delta_{Hom}$ the orbits pass near N^u and jump away near l^o.

4.1. Dynamics in chart K_2. The equilibrium of the homoclinic orbit and the transcritical bifurcation are best described in chart K_2.

In the coordinates of chart K_2 system (3.2) has the form

$$\begin{aligned} J_2' &= r_2 D_2 J_2 \\ D_2' &= r_2(((a-1)H - 1 - a r_2 D_2)J_2 + \Delta_2 - D_2) \\ H' &= r_2(B + r_2\Delta_2 - H - (H+1) r_2 J_2) \\ r_2' &= 0 \\ \Delta_2' &= 0 \end{aligned} \tag{4.1}$$

with time t. System (4.1) is well defined for $r_2 = 0$ and has a trivial flow there because of the common factor r_2. We now desingularize the flow on $\{r_2 = 0\}$ by dividing out the common factor r_2 which corresponds to a rescaling of time $t = r_2 \tilde{t}$ for $r_2 > 0$:

$$\begin{aligned} J_2' &= D_2 J_2 \\ D_2' &= ((a-1)H - 1 - a r_2 D_2)J_2 + \Delta_2 - D_2 \\ H' &= B + r_2\Delta_2 - H - (H+1) r_2 J_2 \\ r_2' &= 0 \\ \Delta_2' &= 0. \end{aligned} \tag{4.2}$$

For $r_2 > 0$ system (4.1) and system (4.2) have the same orbits. For $r_2 = 0$ system (4.2) has a non trivial dynamics now, which provides additional information to describe the dynamics for $r_2 > 0$.

Lemma 2. *System (4.2) has the 2-dimensional manifolds of equilibria*

1. $N_2^s = \{J_2 = 0, D_2 = \Delta_2, H = B + r_2\Delta_2, r_2, \Delta_2\}$ *and*
2. $N_2^u = \{J_2 = \frac{-\Delta_2}{aB - B - 1} + \Delta_2 r_2 O(1), D_2 = 0, H = B + r_2\Delta_2 O(1), r_2, \Delta_2\}$,

parameterized by r_2, Δ_2 small.

Proof: Computation and the Implicit Function Theorem. □

One important feature of these equilibria is the common factor Δ_2 for J_2. We describe the dynamics near the intersection of N_2^u and N_2^s at $\Delta_2 = 0$ first:

Proposition 1. *The equilibrium*

$$o_2 := \{J_2 = 0, D_2 = 0, H = B, r_2 = 0, \Delta_2 = 0\}$$

of system (4.2) has:

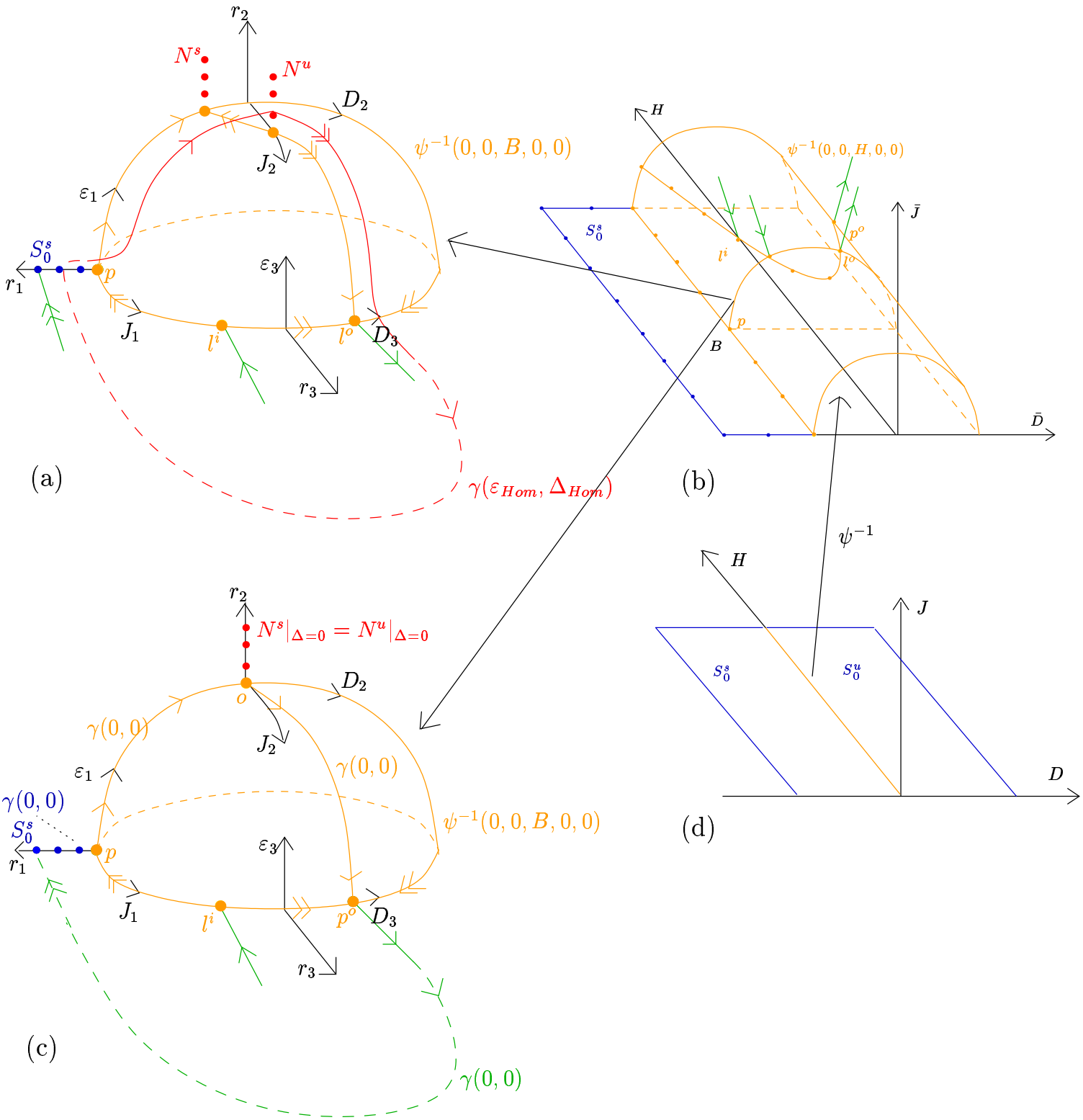

FIG. 4.1. *Blow-up of the laser equations*

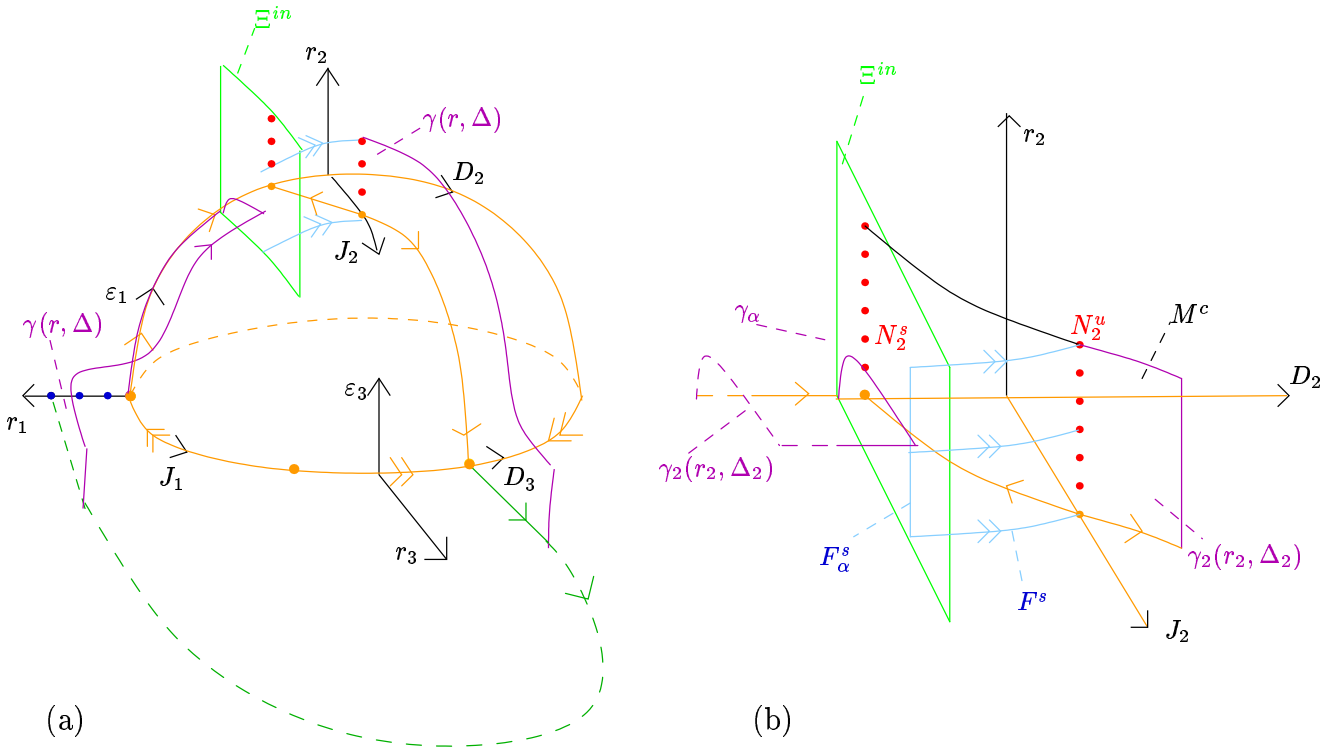

FIG. 4.2. *The manifolds F^s and $\gamma_2(r_2,\Delta_2)$ for $\Delta_2 = \tilde{\Delta}_2 < 0$ (a) in the blow-up picture, (b) the intersection with Ξ^{in}.*

1. *a 3-dimensional center manifold M^c corresponding to the eigenvalue 0 with eigenvectors $(\frac{1}{aB-B-1},1,0,0,0)^T,(0,0,0,1,0)^T,(0,1,0,0,1)^T$,*
2. *a 2-dimensional stable manifold M^s corresponding to the eigenvalue -1 with eigenvectors $(0,1,0,0,0)^T,(0,0,1,0,0)^T$*
3. *and a 2-dimensional stable foliation F^s over M^c with a contraction rate of $O(e^{-ct})$ with a $c \approx 1$.*

Proof: Follows from standard center manifold theory [3, 17]. □
With the transformation

$$\begin{aligned} J_2 &= j_n \\ D_2 &= (aB-B-1)j_n + d_n + \delta_n \\ H &= B + h_n \\ r_2 &= r_n \\ \Delta_2 &= \delta_n \end{aligned} \tag{4.3}$$

we transform system (4.2) to a system with diagonal linear part:

$$\begin{aligned} j_n' &= j_n(j_n(aB-B-1)+d_n+\delta_n) \\ d_n' &= -d_n + j_n O(\|(j_n,d_n,h_n,r_n,\delta_n)\|) \\ h_n' &= -h_n - r_n j_n(B+1+h_n) + r_n\delta_n \\ r_n' &= 0 \\ \delta_n' &= 0. \end{aligned} \tag{4.4}$$

Lemma 3. *The 3-dimensional center manifold of system (4.4) in o has the following struc-*

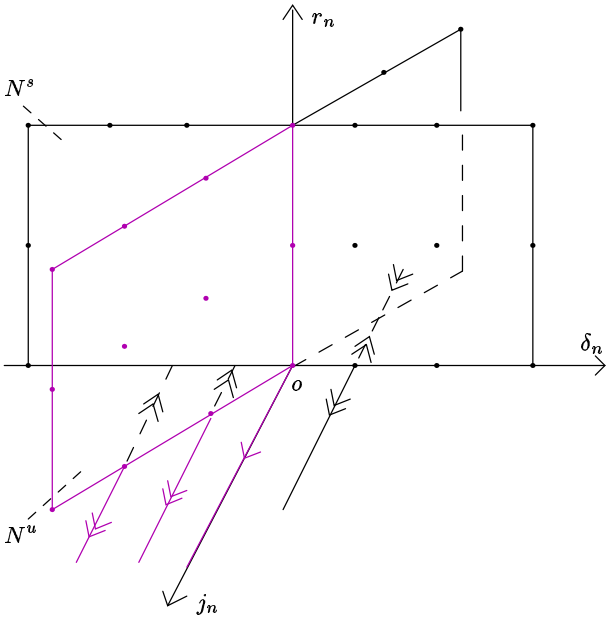

FIG. 4.3. *Dynamics in the center manifold in chart* K_2

ture

$$d_n = d(j_n, r_n, \delta_n) = j_n O(\|(j_n, r_n, \delta_n)\|)$$
$$h_n = h(j_n, r_n, \delta_n) = j_n r_n O(1) + r_n \delta_n.$$

Proof: According to standard center manifold theory ([3, 17]) the 3-dimensional center manifold can be described as a C^k graph over (j_n, r_n, δ_n):

$$d_n = d(j_n, r_n, \delta_n) = O(\|(j_n, r_n, \delta_n)\|^2)$$
$$h_n = h(j_n, r_n, \delta_n) = O(\|(j_n, r_n, \delta_n)\|^2).$$

Since for $j_n = 0$ the center manifold becomes trivial: $d(0, r_n, \delta_n) = 0, h(0, r_n, \delta_n) = r_n \delta_n$ and $h(j_n, 0, \delta_n) = 0$, the assertions follow. □

The dynamics restricted to the center manifold is described by

$$\begin{aligned} j_n' &= j_n(j_n(aB - B - 1) + j_n O(\|(j_n, r_n, \delta_n)\|) + \delta_n) \\ r_n' &= 0 \\ \delta_n' &= 0. \end{aligned} \tag{4.5}$$

which has the manifolds of equilibria N_2^s and N_2^u which are given in these coordinates by

$$N_2^s = \{j_n = 0\}, \tag{4.6}$$
$$N_2^u = \{j_n = \frac{-\delta_n}{aB - B - 1} + \delta_n r_n O(1)\}. \tag{4.7}$$

Lemma 4. *For each small* $r_n > 0$ *a transcritical bifurcation of system (4.5) occurs at* $\delta_n = 0$. *For* $\delta_n < 0$ N_2^s *is stable and* N_2^u *is unstable. The equilibria exchange stability as* δ_n *passes through* 0 *(see Fig. 4.3).*

To describe the behaviour of the full system, we use the dynamics on the center manifold together with the stable foliation F^s over the center manifold. Because r_n and δ_n are constant, we draw the behaviour for certain values in Fig.4.4 in the original coordinates of

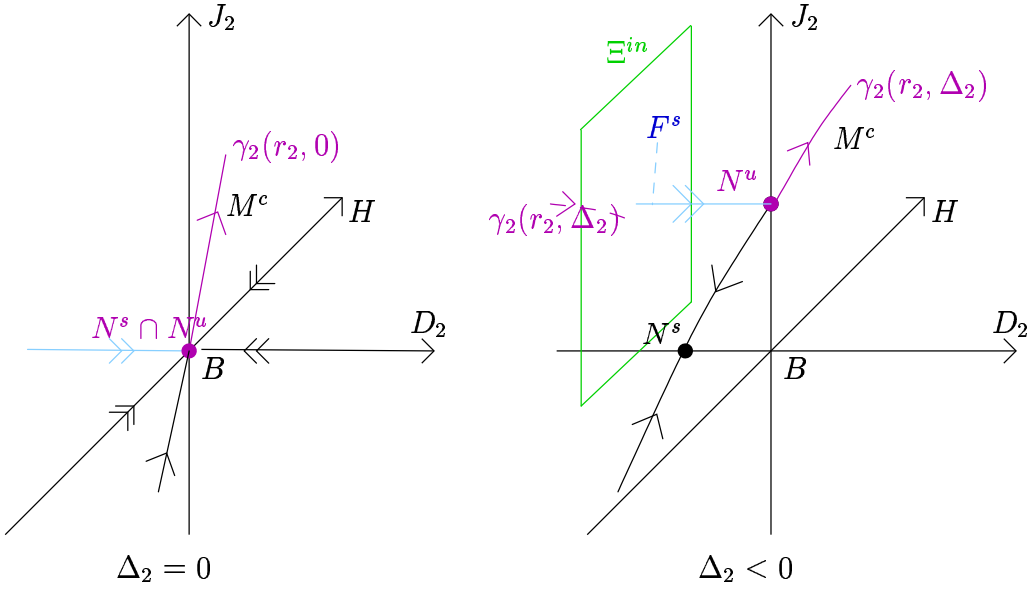

FIG. 4.4. *Center manifold and stable foliation in chart K_2 with a constant $r_2 \geq 0$.*

chart K_2. Near the center manifold the stable manifold M^s of N_2^u consists of the the stable fibres F^s with basepoints in N_2^u.

Next we describe the intersection of the stable manifold M^s with the manifold

$$\Xi^{in} := \{D_2 = -\alpha\}$$

with a small constant α.

Proposition 2. *The stable fibers over the equilibria N_2^u can be parameterized by*

$$\begin{pmatrix} j_n \\ d_n \\ h_n \\ r_n \\ \delta_n \end{pmatrix} = \begin{pmatrix} \delta_n(\frac{-1}{aB-B-1} + \overline{f}_1(d_s, h_s, r_c, \delta_c)) \\ d_s \\ h_s \\ r_c \\ \delta_c \end{pmatrix}$$

with a C^{k-1} function $\overline{f}_1 = O(\|(d_s, h_s, r_c, \delta_c)\|)$.

Proof: It is possible to write the foliation as [3]

$$\begin{pmatrix} j_n \\ d_n \\ h_n \\ r_n \\ \delta_n \end{pmatrix} = \begin{pmatrix} j_c \\ 0 \\ 0 \\ r_c \\ \delta_c \end{pmatrix} + \begin{pmatrix} f_1(j_c, d_s, h_s, r_c, \delta_c) \\ d_s \\ h_s \\ f_4(j_c, d_s, h_s, r_c, \delta_c) \\ f_5(j_c, d_s, h_s, r_c, \delta_c) \end{pmatrix}$$

with f_i a C^k function of order $O(\|(j_c, d_s, h_s, r_c, \delta_c)\|^2)$. Since r_n and δ_n are constant $f_4 = 0$ and $f_5 = 0$. For $j_c = 0$ the flow of (4.4) and the fibers are trivial,

$$f_1(0, d_s, h_s, r_c, \delta_c) = 0, \ \forall d_s, h_s, r_c, \delta_c.$$

Therefore

$$f_1(j_c, d_s, h_s, r_c, \delta_c) = j_c \tilde{f}_1(j_c, d_s, h_s, r_c, \delta_c)$$

with a C^{k-1} function $\tilde{f}_1 = O(\|(j_c, d_s, h_s, r_c, \delta_c)\|^0)$ and $j_n = j_c(1 + \tilde{f}_1)$. On the center manifold there is $d_s = d(j_c, r_c, \delta_c), h_s = h(j_c, r_c, \delta_c)$ (see Lemma 3) and $\tilde{f}_1 = 0$. So we

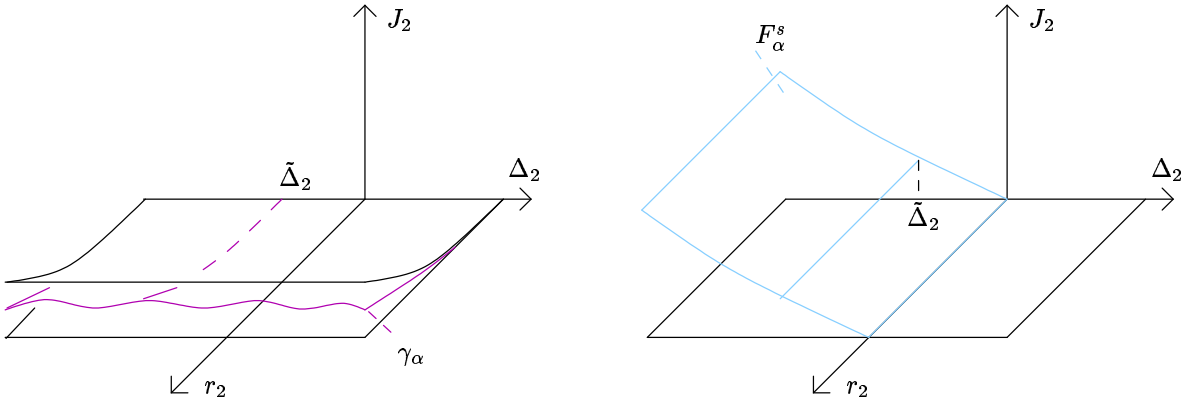

FIG. 4.5. *The manifolds F^s_α and $\gamma_\alpha(r_2, \Delta_2)$ in Ξ^{in}*

get $\tilde{f}_1 = O(\|(j_c, d_s, h_s, r_c, \delta_c)\|^1)$. The coordinates j_c, r_c, δ_c, of the center manifold, follow the dynamics of (4.5). Because we are interested in fibers over N_2^u (4.7) we can substitute $j_c = \frac{-\delta_c}{aB-B-1} + \delta_c r_c O(1)$ and get

$$j_n = \delta_c\left(\frac{-1}{aB - B - 1} + \overline{f}_1(d_s, h_s, r_c, \delta_c)\right)$$

with a C^{k-1} function $\overline{f}$ of order $O(\|(d_s, h_s, r_c, \delta_c)\|)$. □

Theorem 2. *The intersection of the fibers with Ξ^{in} in original coordinates is (see Fig. 4.5):*

$$\begin{pmatrix} J_2 \\ D_2 \\ H \\ r_2 \\ \Delta_2 \end{pmatrix} = \begin{pmatrix} \delta_n(\frac{-1}{aB-B-1} + \overline{f}_1(-\alpha + O(\delta_n), h_n, r_n, \delta_n)) \\ -\alpha \\ B + h_n \\ r_n \\ \delta_n \end{pmatrix}.$$

Proof: Transforming to the original coordinates of K_2 gives

$$\begin{pmatrix} J_2 \\ D_2 \\ H \\ r_2 \\ \Delta_2 \end{pmatrix} = \begin{pmatrix} \delta_n(\frac{-1}{aB-B-1} + \overline{f}_1(d_n, h_n, r_n, \delta_n)) \\ \delta_n(\overline{f}_1(d_n, h_n, r_n, \delta_n)(aB - B - 1) + d_n) \\ B + h_n \\ r_n \\ \delta_n \end{pmatrix}.$$

Because $D_2 = -\alpha$ in Ξ^{in} we can solve this equation according to the Implicit Function Theorem in $\delta_n = 0$ for d_n and get $d_n = -\alpha + \delta_n O(\|(\alpha, h_n, r_n, \delta_n)\|)$. Substitution of d_n into the first equation gives the statement. □

We start by describing the part of the manifold $\gamma_2(r_2, \Delta_2)$ corresponding to the local unstable manifolds M^u of the equilibria N_2^u. Following our convention we denote the unstable manifold of the equilibria N_2^u by $\gamma_2(r_2, \Delta_2)$, where subscript $_2$ indicates that we are working in chart K_2. The outgoing orbits lie in the center manifold M^c. We define the outgoing section of chart K_2, which intersects the unstable manifold M^u transversally, by

$$\Xi^{out} = \{J_2 = \alpha\}$$

with $\alpha > 0$ as above. We get:

Theorem 3. *The intersection of* Ξ^{out} *and* $\gamma_2(r_2, \Delta_2)$ *is given by*

$$\begin{pmatrix} J_2 \\ D_2 \\ H \\ r_2 \\ \Delta_2 \end{pmatrix} = \begin{pmatrix} \alpha \\ ((aB - B - 1) + O(\|(\alpha, r_n, \delta_n)\|))\alpha + \Delta_2 \\ B + r_2 O(\|(\alpha, r_n, \delta_n)\|) \\ r_n \\ \Delta_n \end{pmatrix}$$

with $D_2 = D_2(r_2, \Delta_2) > 0$ *and* $H = H(r_2, \Delta_2) = B + r_2 O(\|(\alpha, r_2, \Delta_2)\|)$.
Proof: Because r_n and δ_n are constant, the unstable manifold for $\delta_n \leq 0$ of the equilibria N_2^u of equation (4.5) can be described by

$$j_n > \delta_n(\frac{-1}{aB - B - 1} + O(\|(r_n, \delta_n)\|)).$$

The other variables are (Lemma 3)

$$\begin{aligned} d_n &= j_n O(\|(j_n, r_n, \delta_n)\|) \\ h_n &= j_n r_n O(1). \end{aligned}$$

The transformation (4.3) to the original coordinates of chart K_2 and setting $j_n = \alpha$ proves the Theorem. □

Next we follow $\gamma_2(r_2, \Delta_2)$ through the region $\{J_2 > 0\}$. We choose to describe the dynamics in chart K_3, which has certain computational advantages.

4.2. Dynamics in chart K_3 near the exit point. The change of coordinates from chart K_2 to chart K_3, which is a diffeomorphism from $\{J_2 > 0, r_2 > 0\}$ to $\{\varepsilon_3 > 0, r_3 > 0\}$, is given by

$$r_3 = r_2 J_2^{1/2},\ D_3 = J_2^{-1/2} D_2,\ \varepsilon_3 = J_2^{-1/2},\ \Delta_3 = J_2^{-1/2}\Delta_2.$$

The outgoing section in chart K_2, Ξ^{out}, is mapped to the incoming section of chart K_3, Σ_3^{in}, defined by

$$\Sigma_3^{in} := \{\varepsilon_3 = \alpha^{-1/2}\}.$$

In chart K_3 the manifold $\gamma_2(r_2, \Delta_2)$ is described by $\gamma_3(r_3, \Delta_3)$:
Lemma 5. *For sufficiently small* Δ_3, r_3 *the manifold* γ_3 *has the following parametrisation in* Σ_3^{in}*:*

$$D_3 = \tilde{D}(r_3, \Delta_3),\ H = B + r_3\tilde{H}(r_3, \Delta_3)$$

with C^k*-functions* $\tilde{D}$ *and* $\tilde{H}$ *(see Fig. 4.6).*

The dynamics in chart K_3 is given by

$$\begin{aligned} r_3' &= \frac{1}{2} r_3 D_3 \\ D_3' &= (a-1)H - 1 - a r_3 D_3 + \varepsilon_3(\Delta_3 - D_3) - \frac{1}{2} D_3^2 \\ H' &= -(H+1)r_3 + \varepsilon_3(B + r_3\Delta_3 - H) \\ \varepsilon_3' &= -\frac{1}{2}\varepsilon_3 D_3 \\ \Delta_3' &= -\frac{1}{2}\Delta_3 D_3, \end{aligned} \tag{4.8}$$

after dividing out the common factor r_3. This system has the invariant manifolds $\{r_3 = 0\}$, $\{\varepsilon_3 = 0\}$, and $\{\Delta_3 = 0\}$. Further it has the curve of equilibria

$$l_3^o := \{r_3 = 0,\ D_3 = \sqrt{2((a-1)H - 1)},\ H,\ \varepsilon_3 = 0,\ \Delta_3 = 0\}$$

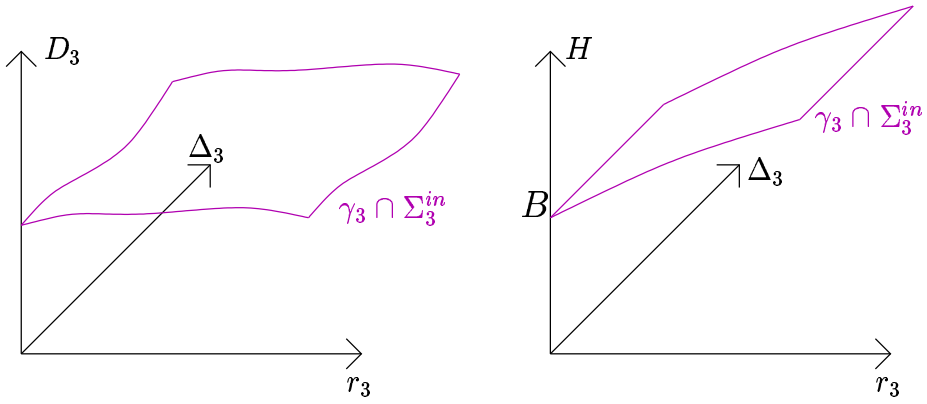

FIG. 4.6. *The manifold* $\gamma_3(r_3, \Delta_3)$ *in* Σ^3_{in}

which are the 'exit' points of the cylinder $\{r_3 = 0\}$. (The curve of 'exit' points is attracting to orbits in $\{r_3 = 0\}$ at least locally and repelling in the direction of $r_3 > 0$. Therefore orbits with $r_3 > 0$, which pass nearby, jump away from $\{r_3 = 0\}$ close to l_3^o.) The other curve of equilibria,

$$l_3^i := \{r_3 = 0,\ D_3 = -\sqrt{2((a-1)H-1)},\ H,\ \varepsilon_3 = 0,\ \Delta_3 = 0\},$$

corresponds to the 'entrance' points. The manifold of unstable equilibria from chart K_2, N_2^u, has the parametrisation

$$N_3^u := \{r_3 = \varepsilon_3 \frac{B-H}{H+1-\Delta_3\varepsilon_3},\ D_3 = 0,\ H,\ \varepsilon_3,\ \Delta_3 = \frac{H+1-aH}{\varepsilon_3}\}.$$

Near the equilibrium p_3^o,

$$p_3^o := l_3^o \cap \{H = B\},$$

which satisfies $\{D = D_o := \sqrt{aB - B - 1}\}$ we have the following invariant manifolds:

Proposition 3. *In* p_3^o *system (4.8) has*

1. *a 4-dimensional center-stable manifold* $M^{cs} \subseteq \{r_3 = 0\}$, *which consists of a 3-dimensional stable manifold* $M^s \subseteq \{r_3 = 0,\ H = B\}$ *corresponding to the eigenvalues* $-D_0$, $-\frac{1}{2}D_0$ *and* $-\frac{1}{2}D_0$ *and a 1-dimensional center manifold* M^c *corresponding to the eigenvalue* 0, *which is the line of equilibria* l_3^o,
2. *a 1-dimensional unstable manifold* M^u *corresponding to the eigenvalue* $\frac{1}{2}D_0$ *transversal to* $\{r_3 = 0\}$.

Proof: Standard center manifold theory □

Let

$$\Sigma_3^e := \{\varepsilon_3 = e\},$$

$$\Sigma_3^{out} := \{r_3 = \rho\}$$

be sections near p^o with sufficiently small $e, \rho > 0$. Further the intersection of the unstable manifold M^u with Σ_3^{out} defines

$$q^o := M^u \cap \Sigma_3^{out}.$$

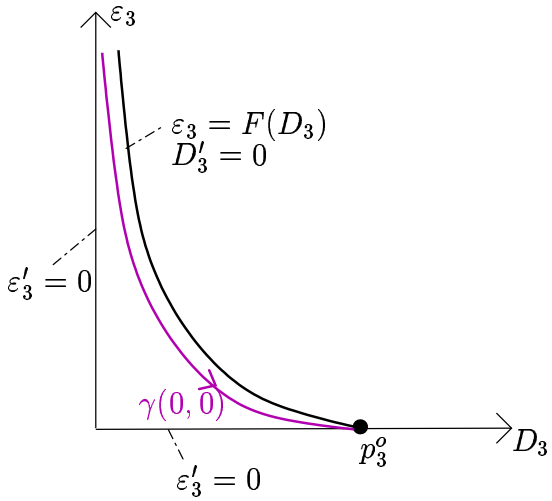

FIG. 4.7. *Dynamics of system (4.9)*

4.2.1. Transition from Σ_3^{in} to Σ_3^e. In Σ_3^{in} the singular homoclinic orbit $\gamma_3(0,0)$ is part of the invariant manifold $\{r_3 = 0, H = B, \Delta_3 = 0\}$ of system (4.8). Therefore we look at the subsystem:

$$\begin{aligned} D_3' &= aB - B - 1 - \varepsilon_3 D_3 - \frac{1}{2} D_3^2 \\ \varepsilon_3' &= -\frac{1}{2}\varepsilon_3 D_3. \end{aligned} \tag{4.9}$$

Lemma 6. *The singular homoclinic orbit $\gamma_3(0,0)$ converges to p_3^o as $t \to \infty$ (see Fig. 4.7).*
Proof: The vector field of system (4.9) has the following properties

- $\varepsilon_3' = 0$ for $\varepsilon_3 = 0$ or $D_3 = 0$ and $\varepsilon_3' < 0$ for $\varepsilon_3, D_3 > 0$,
- $D_3' = 0$ for $\varepsilon_3 = F(D_3)$, $D_3' < 0$ for $\varepsilon_3 < F(D_3)$, and $D_3' > 0$ for $\varepsilon_3 > F(D_3)$,

where $F(D_3) := \frac{-D_3/2 + aB - B - 1}{D_3}$. Therefore the region

$$C := \{D_3 \geq 0, 0 \leq \varepsilon \leq F(D_3)\}$$

is positive invariant under the flow and all orbits in C converge to p_3^o. The D_3 coordinates of the orbit $\gamma(0,0)$ satisfies $D_3 > 0$ and $D_3' > 0$ for ε_3 sufficiently large because $\gamma(0,0)$ starts as the unstable manifold to o in the center manifold of chart K_2. So we get $\gamma(0,0) \in C$ and the assertion follows. □

Lemma (6) implies that $\gamma(0,0)$ needs a finite time for the transition from Σ_3^{in} to Σ_3^e. If $r_3, \Delta_3 > 0$ in Σ_3^{in} are sufficiently small, $\gamma_3(r_3, \Delta_3)$ is a small perturbation from $\gamma(0,0)$ and the map from Σ_3^{in} to Σ_3^e is a diffeomorphism.

We denote by subscript $_i$ the initial values in Σ_3^e and by subscript $_o$ the variables in Σ_3^{out}. We get:

Lemma 7. *The manifold γ_3 in Σ_3^e is described by*

$$\begin{aligned} D_3 &= D_i(r_i, \Delta_i) = d^*(r_i, \Delta_i) \\ H &= H_i(r_i, \Delta_i) = B + r_i h^*(r_i, \Delta_i) \end{aligned}$$

with C^k functions d^*, h^*.

4.2.2. Dynamics near the non-hyperbolic equilibrium p_3^o. We need to describe the transition $\Pi : \Sigma_3^e \to \Sigma_3^{out}$,

$$(r_o, D_o, H_o, \varepsilon_o, \Delta_o) = \Pi(r_i, D_i, H_i, \varepsilon_i, \Delta_i),$$

of γ_3 near the equilibrium p_3^o. We need to show that $\gamma_3 \cap \Sigma_3^{out}$ is a 2-dimensional smooth manifold with some bounds on the derivatives. We cannot apply the techniques used in [22] to analyze the dynamics near the exit point, because p_3^o is a non-hyperbolic equilibrium. Nor we can use the transformation to a certain standard form for partially hyperbolic equilibria described by Takens [25] because of the resonances of the eigenvalues.

Instead we use Fenichel coordinates [19] to transform our system to the form

$$\begin{aligned} x_s' &= \Lambda(x_s, x_u, x_c)x_s \\ x_u' &= \Gamma(x_s, x_u, x_c)x_u \\ x_c' &= h(x_c) + H(x_s, x_u, x_c) \otimes x_s \otimes x_u. \end{aligned} \tag{4.10}$$

(Here $x_c \in \mathbb{R}^{n_c}$, $x_s \in \mathbb{R}^{n_s}$, $x_u \in \mathbb{R}^{n_u}$ describe the center, stable or unstable directions and $h \in \mathbb{R}^{n_c}$, $\Lambda \in \mathbb{R}^{n_s} \times \mathbb{R}^{n_s}$, $\Gamma \in \mathbb{R}^{n_u} \times \mathbb{R}^{n_u}$ are C^k, and H ($\in C^k$) is a rank three tensor with $\otimes$ denoting the tensor product.)

It will be important in later calculations that the H coordinate of $\gamma_3 \cap \Sigma_3^e$ has the same form after the transformation to Fenichel coordinates and normal form transformations as in Lemma 7.

The first step (for $H > \frac{a}{a-1}$) is

$$D_3 = \sqrt{2((a-1)H - 1)} + \tilde{d}, H = B + \tilde{h}$$

which shifts the curve of equilibria to $r_3 = \tilde{d} = \varepsilon_3 = \Delta_3 = 0$ and only changes the equation for $\tilde{d}$. Because $D_3 = \sqrt{2(aB - B - 1 + (a-1)\tilde{h})} + \tilde{d} \neq 0$ near $H = B$ we can divide the right-hand side of (4.8) by D_3 which again corresponds to a space dependent time transformation. This simplifies the first, fourth and fifth equation. For the other two equations we develop D_3^{-1} into a series

$$D_3^{-1} = \frac{1}{D_0} \frac{1}{1 + O(\|(\tilde{d}, \tilde{h})\|)} = \frac{1}{D_0}(1 + O(\|(\tilde{d}, \tilde{h})\|)$$

which simplifies the linear terms and adds some higher order terms. Multiplying our system with D_3^{-1} means changing the Jacobian at the origin by a common factor $\frac{1}{D_0}$. To transform our system to diagonal form we use the transformation

$$\begin{pmatrix} r_3 \\ \tilde{d} \\ \tilde{h} \\ \varepsilon_3 \\ \Delta_3 \end{pmatrix} = \begin{pmatrix} 1 & 0 & 0 & 0 & 0 \\ \frac{-2(aD_0^2 + 2a(B+1) - 2(B+1)) + 6(B+1)(a-1)D_0}{3D_0^3} & 1 & \frac{a-1-(a-1)D_0}{D_0^2} & 1 & 0 \\ \frac{-2(B+1)}{D_0} & 0 & 1 & 0 & 0 \\ 0 & 0 & 0 & 1 & 0 \\ 0 & 0 & 0 & 0 & 1 \end{pmatrix} \begin{pmatrix} r_d \\ d_d \\ h_d \\ \varepsilon_d \\ \delta_d \end{pmatrix}$$

and we finally get a system of the form

$$\begin{aligned} r_d' &= \frac{1}{2} r_d \\ d_d' &= -d_d + O(2) \\ h_d' &= \varepsilon_d O(1) + r_d O(1) \\ \varepsilon_d' &= -\frac{1}{2}\varepsilon_d \\ \Delta_d' &= -\frac{1}{2}\Delta_d, \end{aligned} \tag{4.11}$$

where $O(n)$ denotes C^k functions of order $O(\|(r_d, d_d, h_d, \varepsilon_d, \Delta_d)\|^n)$. So far the general form has not changed for γ_3 in Σ_3^e, there still exist some C^k functions d^*, h^* such that $d_d = d^*(r_d, \Delta_d)$, $h_d = r_d h^*(r_d, \Delta_d)$.

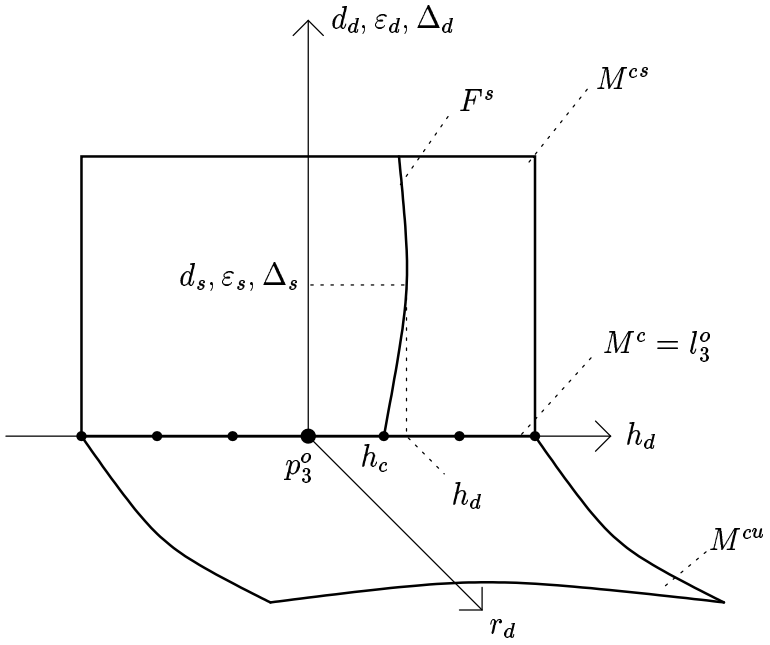

FIG. 4.8. *Invariant manifolds and foliation of system (4.11)*

Following the steps of the transformation to Fenichel coordinates described in [19], we first straighten out the center-stable and center-unstable manifolds and afterwards straighten out the fibers in these two manifolds (see Fig. 4.8). We are interested in which way the higher order terms are changed by the transformation to obtain the form of the initial conditions. We finally get:

Theorem 4. *In Fenichel coordinates, system (4.8) has the form*

$$\begin{aligned} r' &= \frac{1}{2}r \\ d' &= -d + \Lambda(r,d,h,\varepsilon,\Delta)\cdot(d,\varepsilon,\Delta)^T \\ h' &= H(r,d,h,\varepsilon,\Delta)\cdot(d,\varepsilon,\Delta)^T r \\ \varepsilon' &= -\frac{1}{2}\varepsilon \\ \Delta' &= -\frac{1}{2}\Delta, \end{aligned} \tag{4.12}$$

with the initial conditions in Σ_3^e*:*

$$r = r_i, d = d_i = d^*(r_i,\Delta_i), h = h_i = r_i h^*(r_i,\Delta_i),$$

and $\Lambda \in C^{k-2}$ *of order* $O(1)$*,* $H \in C^{k-3}$ *of order* $O(0)$*,* $d^* \in C^{k-1}$ *and* $h^* \in C^{k-2}$*, both of order* $O(0)$*. Here again* $O(n)$ *denotes functions of order* $O(\|(r_d,d_d,h_d,\varepsilon_d,\Delta_d)\|^n)$*.*

4.2.3. Transition from Σ_3^e to Σ_3^{out}. For the transition time T of the transition from Σ_3^e to Σ_3^{out} we get:

Lemma 8. *The transition time* T *is*

$$T = 2ln(\frac{\rho}{r_i}).$$

The transition from $\Sigma_3^e \cap \{r \geq c\}$ to Σ_3^{out} is a diffeomorphism for each small $c > 0$. We use the special form of the Fenichel coordinates together with Gronwall-like-estimates to get bounds of the coordinates $d(t), h(t)$ of γ_3 during the transition. Afterwards

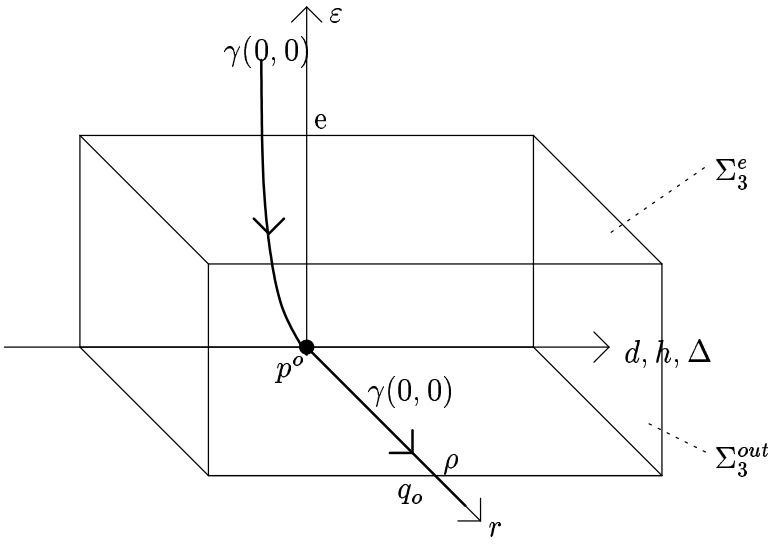

FIG. 4.9. *The singular orbit* $\gamma(0,0)$ *in Fenichel coordinates near* p^o.

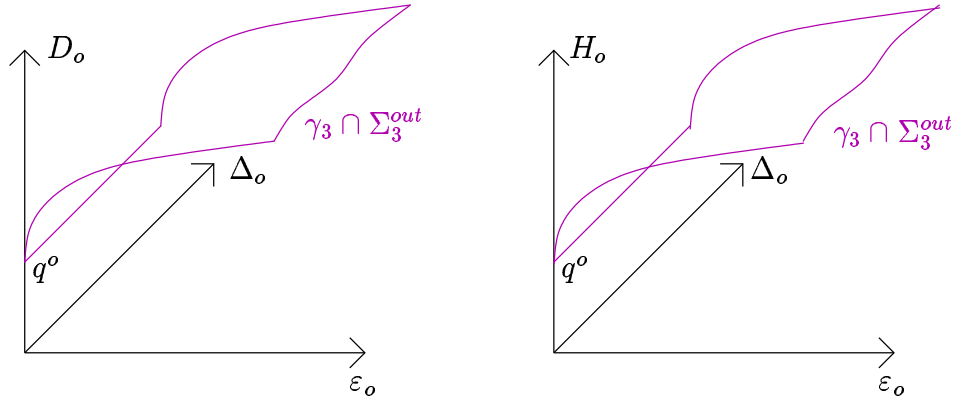

FIG. 4.10. *Intersection of* γ_3 *with* Σ_3^{out}

we use variational equations to obtain bounds for $\frac{\partial}{\partial \Delta_i} d(t)$, $\frac{\partial}{\partial \Delta_i} h(t)$, $\frac{\partial}{\partial r_i} d(t)$, and $\frac{\partial}{\partial r_i} h(t)$ in a similar way. We finally get:

Proposition 4. *For* r_i, Δ_i *small enough* $\gamma_4(r_i, \Delta_i) \cap \Sigma_3^{out}$ *satisfies*

$$d(T) = O(r_i), \quad \frac{\partial}{\partial \Delta_i}(d(T)) = O(r_i), \quad \frac{\partial}{\partial r_i}(d(T)) = O(r_i^0)$$
$$h(T) = O(r_i ln(r_i)), \frac{\partial}{\partial \Delta_i}(h(T)) = O(r_i ln(r_i)), \frac{\partial}{\partial r_i}(h(T)) = O(ln(r_i)).$$

Proof: Because the proof of this proposition is very technical it is performed in the Appendix. □

The combination of the coordinate transformation from the coordinates of chart K_3, $(r_3, D_3, H, \varepsilon_3, \Delta_3)$, to the final coordinates in Fenichel normal form with some steps of normal form transformation, $(r, d, h, \varepsilon, \Delta)$, is a C^{k-3} diffeomorphism:

$$r_3 = r, D_3 = \Phi_1(r, d, h, \varepsilon, \Delta), H = \Phi_2(r, d, h, \varepsilon, \Delta), \varepsilon_3 = \varepsilon, \Delta_3 = \Delta.$$

For $r = 0$ the intersection of $\gamma(0,0)$ with Σ_3^{out}, which is equal to $q_3^o = M^u \cap \Sigma_3^{out}$ is

$$(r, d, h, \varepsilon, \Delta) = (\rho, 0, 0, 0, 0),$$

which is in the original coordinates of K_3

$$q_3^o = (\rho, \Phi_1(\rho, 0, 0, 0, 0), \Phi_2(\rho, 0, 0, 0, 0), 0, 0)^T.$$

The transformation back to the original coordinates of chart K_3 yields:
Theorem 5. *For the intersection of γ_3 with Σ_3^{out} we get*

$$\begin{pmatrix} r_o \\ D_o \\ H_o \\ \varepsilon_o \\ \Delta_o \end{pmatrix} = q^o + \begin{pmatrix} 0 \\ D_*(\varepsilon_o, \Delta_o) \\ H_*(\varepsilon_o, \Delta_o) \\ \varepsilon_o \\ \Delta_o \end{pmatrix},$$

where D_*, H_* are C^{k-3} for $\varepsilon > 0$, which satisfy

$$D_*(\varepsilon_o, \Delta_o) = O(\varepsilon_o ln(\varepsilon_o)),\ H_*(\varepsilon_o, \Delta_o) = O(\varepsilon_o ln(\varepsilon_o))$$

and

$$\frac{\partial}{\partial \varepsilon_o} D_* = O(ln(\varepsilon_o)),\ \frac{\partial}{\partial \varepsilon_o} H_* = O(ln(\varepsilon_o)),\ \frac{\partial}{\partial \Delta_o} D_* = O(ln(\varepsilon_o)),\ \frac{\partial}{\partial \Delta_o} H_* = O(ln(\varepsilon_o)).$$

for $\varepsilon_o \to 0$.
Proof: We can write the transformations Φ_i as

$$D_3 = \Phi_1(r, 0, 0, 0, 0) + A_1(r, d, h, \varepsilon, \Delta)(d, h, \varepsilon, \Delta)^T$$

$$H = \Phi_2(r, 0, 0, 0, 0) + A_2(r, d, h, \varepsilon, \Delta)(d, h, \varepsilon, \Delta)^T$$

with two functions $A_1, A_2 \in C^{k-3}(\mathbb{R}^5, \mathbb{R}^4)$. We get in Σ_3^{out} that

$$\begin{aligned} \Phi_i(\rho, d, h, \varepsilon, \Delta) - \Phi_i(\rho, 0, 0, 0, 0) &= A_1(\rho, d, h, \varepsilon, \Delta)(O(r_i), O(r_i ln(r_i)), O(r_i), O(r_i)) \\ &= O(r_i ln(r_i)). \end{aligned}$$

The bounds on the derivatives are

$$\frac{\partial}{\partial \Delta_i} \Phi_i(\rho, d, h, \varepsilon, \Delta) = O(r_i ln(r_i)),\ \frac{\partial}{\partial r_i} \Phi_i(\rho, d, h, \varepsilon, \Delta) = O(ln(r_i)).$$

So we have in Σ_3^{out}:

$$\begin{pmatrix} r_o \\ D_o \\ H_o \\ \varepsilon_o \\ \Delta_o \end{pmatrix} = q^o + \begin{pmatrix} 0 \\ O(r_i ln(r_i)) \\ O(r_i ln(r_i)) \\ e r_i/\rho \\ \Delta_i r_i/\rho \end{pmatrix}.$$

Changing the parametrisation to $\varepsilon_o = \frac{e r_i}{\rho}, \Delta_o = \frac{\Delta_i r_i}{\rho}$ we get the statement of this theorem because of

$$\frac{\partial}{\partial \varepsilon_o} D_3 = \frac{\partial D_3}{\partial r_i} \frac{\rho}{e} + \frac{\partial D_3}{\partial \Delta_i} \frac{-\Delta_i}{\varepsilon_o},\ \frac{\partial}{\partial \Delta_o} D_3 = \frac{\partial D_3}{\partial \Delta_i} \frac{e}{\varepsilon_o}.$$

□

4.3. Jump to the slow manifold S_ε^s . We now describe how the manifold γ jumps from the neighbourhood of the non-hyperbolic line close to the stable part of the slow manifold S_ε^s. Here it is convenient to go back to the original variables (J, D, H) and parameters (ε, Δ). The transformation

$$J_{out} = \rho^2,\ D_{out} = \rho D_o,\ H_{out} = H_o,\ \varepsilon = \rho\varepsilon_o,\ \Delta = \rho\Delta_o$$

of $\gamma_3 \cap \Sigma_3^{out}$ back to the original coordinates before the blow up shows that $\gamma \cap \Sigma_3^{out}$ can be parameterized by

$$J_{out} = \rho^2, D_{out} = D_{out}(\varepsilon, \Delta), H_{out} = H_{out}(\varepsilon, \Delta)$$

where $D_{out}, H_{out} \in C^{k-3}$ for $\varepsilon > 0$ and the partial derivatives with respect to ε, Δ are of order $O(ln(\varepsilon))$ for $\varepsilon \to 0$. The map describing the jump back from Σ_3^{out} to the transverse section

$$\Sigma^{in} := \{J = \rho^2\}$$

lying near the stable part of the slow manifold S_ε^s close to the solutions of the layer problem is a C^k diffeomorphism:

$$D = \Psi_1(D_{out}, H_{out}, \varepsilon, \Delta),\ H = \Psi_2(D_{out}, H_{out}, \varepsilon, \Delta).$$

For $\varepsilon = 0$ the jump back and D_{out}, H_{out} are independent of Δ and

$$\Psi_i(D_{out}(0, \Delta), H_{out}(0, \Delta), 0, \Delta) = \Psi_i(D_{out}(0, 0), H_{out}(0, 0), 0, 0),$$

and $q_i := \Psi(q^o)$. Because in chart K_3 the inequality $D_3 \geq c > 0$ is satisfied, we get that $D \geq \rho c > 0$. Therefore $\gamma \cap \Sigma^{in}$ satisfies $D \leq -\tilde{c} < 0$ for some constant $\tilde{c} > 0$, which means that γ returns close to a vicinity of the stable manifolds S_ε^s with a nonzero distance to the not normally hyperbolic line L of at least $\tilde{c}$.

This implies:

Theorem 6. *The intersection of γ with Σ^{in} is given by*

$$J_i = \rho^2,\ D_i = D(\varepsilon, \Delta),\ H_i = H(\varepsilon, \Delta)$$

with $D(\varepsilon, \Delta)$ and $H(\varepsilon, \Delta)$ are C^{k-3} for $\varepsilon > 0$ and continuous on $\varepsilon \geq 0$ with

$$\frac{\partial}{\partial\varepsilon}D = O(ln(\varepsilon)),\ \frac{\partial}{\partial\varepsilon}H = O(ln(\varepsilon)),\ \frac{\partial}{\partial\Delta}D = O(ln(\varepsilon)),\ \frac{\partial}{\partial\Delta}D = O(ln(\varepsilon)).$$

Additionally, we have $D_i \leq -\tilde{c} < 0$ for some constant $\tilde{c} > 0$.

4.4. Exponential attraction to the slow manifold S_ε^s. We now study the evolution of γ as it drifts slowly along the stable part of the slow manifold S_ε^s. Here it is again convenient to use the original variables (J, D, H) and parameters (ε, Δ).

For $\rho < \tilde{c}$, where $\tilde{c}$ has been introduced in the previous subsection, we describe the transition from Σ^{in} to

$$\Sigma^{out} := \{D = -\rho\}.$$

Theorem 7. $\gamma \cap \Sigma^{out}$ *satisfies the relations*

$$J_o = J_o(\varepsilon, \Delta),\ D_o = -\rho,\ H_o = H_o(\varepsilon, \Delta)$$

with $J_o, H_o \in C^{k-4}$ for $\varepsilon > 0$ and $H_o \in C$, $J_o \in C^1$ for $\varepsilon \geq 0$, satisfying the bounds

$$J_o = O(e^{-c/\varepsilon}),\ \frac{\partial}{\partial\varepsilon}J_o = O(e^{-c/\varepsilon}),\ \frac{\partial}{\partial\Delta}J_o = O(e^{-c/\varepsilon}),$$

$$H_o = O(1),\ \frac{\partial}{\partial\varepsilon}H_o = O(ln(\varepsilon)),\ \frac{\partial}{\partial\Delta}H_o = O(ln(\varepsilon)).$$

Proof: According to Fenichel's theory we have a stable foliation F^s over the slow manifold $S_\varepsilon = \{J = 0\}$. The dynamics separates in a slow drift in direction of the slow manifold and an exponential attraction of order $O(e^{-c/\varepsilon})$ to S_ε along the stable fibers. Because the dynamics in the slow manifold is C^k and the foliation is C^k the transition Π from from Σ^{in} to Σ^{out} is C^k. For

$$(J_o, D_o, H_o, \varepsilon, \Delta) = \Pi(J_i, D_i, H_i, \varepsilon, \Delta)$$

we have:

$$J_o = e^{-c/\varepsilon} j(J_i, D_i, H_i, \varepsilon, \Delta),\ H_o = h(J_i, D_i, H_i, \varepsilon, \Delta),\ D_o = -\rho,$$

with j, h C^k. Because $(J_o)_\varepsilon = e^{-c/\varepsilon} O(ln(\varepsilon))$, $(H_o)_\varepsilon = O(1)O(ln(\varepsilon))$ and analogously for the derivatives with respect to Δ the theorem follows. □

4.5. Dynamics in chart K_1, the incoming flow. In chart K_1 the orbit $\gamma(\varepsilon, \Delta)$ is described by $\gamma_1(\varepsilon_1, \Delta_1)$. It passes near the point p (now p_1) (see Fig. 4.1). We describe the transition of $\gamma_1(\varepsilon_1, \Delta_1)$ from the section

$$\Sigma_1^{in} := \{r_1 = \rho, \varepsilon_1 \in [0, e]\},$$

which corresponds to the section Σ^{out} defined in the previous subsection, to the section

$$\Sigma_1^{out} := \{r_1 \in [0, \rho], \varepsilon_1 = e\},$$

with small constants $\rho, e > 0$. We denote the coordinates in Σ_1^{in} by subscript $_{1i}$ and all coordinates in Σ_1^{out} by subscript $_{1o}$.

The manifold $\gamma_1(\varepsilon_{1i}, \varepsilon_{2i}) \cap \Sigma_1^{in}$ satisfies:

- $J_{1i}(\varepsilon_{1i}, \Delta_{1i})$ is a C^1 function satisfying $J_{1i}(\varepsilon_{1i}, \Delta_{1i}) = O(e^{-c/\varepsilon_{1i}})$ with a constant $c > 0$.
- $H_{1i}(\varepsilon_{1i}, \Delta_{1i})$ is continuous for $\varepsilon_{1i} \geq 0$ and C^1 for $\varepsilon_{1i} > 0$. The derivatives satisfy the bounds:

$$\frac{\partial}{\partial \varepsilon_{1i}} H_{1i} = O(ln(\varepsilon_{1i})),\ \frac{\partial}{\partial \Delta_{1i}} H_{1i} = O(ln(\varepsilon_{1i})).$$

- The parameter Δ_{1i} satisfies $-\frac{\varepsilon_{1i}}{2e} \leq \Delta_{1i} < 0$ and Δ_{1i} sufficiently small if Δ_2 was chosen sufficiently small in chart K_2, which is possible.

After desingularisation by dividing out the common factor r_1, equation (3.2) has the form

$$\begin{aligned} J_1' &= -J_1 + 2J_1 h(J_1, r_1, H, \varepsilon_1, \Delta_1) \\ r_1' &= -r_1 h(J_1, r_1, H, \varepsilon_1, \Delta_1) \\ H' &= -(H+1) r_1 J_1 + \varepsilon_1 (B - H) \\ \varepsilon_1' &= \varepsilon_1 h(J_1, r_1, H, \varepsilon_1, \Delta_1) \\ \Delta_1' &= \Delta_1 h(J_1, r_1, H, \varepsilon_1, \Delta_1), \end{aligned} \tag{4.13}$$

with $h(J_1, r_1, H, \varepsilon_1, \Delta_1)) := ((a-1)H - 1)J_1 + a r_1 J_1 + \varepsilon_1(\Delta_1 + 1)$. The equations for ε_1 and Δ_1 are obtained by differentiation of the defining equations: $\varepsilon' = (r_1 \varepsilon_1)'$ and $\Delta' = (r_1 \Delta_1)'$.

This system has the invariant manifold $\{J_1 = 0\}$, which contains the critical manifold S_0^s in chart K_1:

$$S_{01}^s = \{J_1 = 0, r_1, H, \varepsilon_1 = 0, \Delta_1\}.$$

The other manifold of equilibria

$$N_1^s := \{J_1 = 0, r_1, H = B - r_1, \varepsilon_1, \Delta_1 = -1\}$$

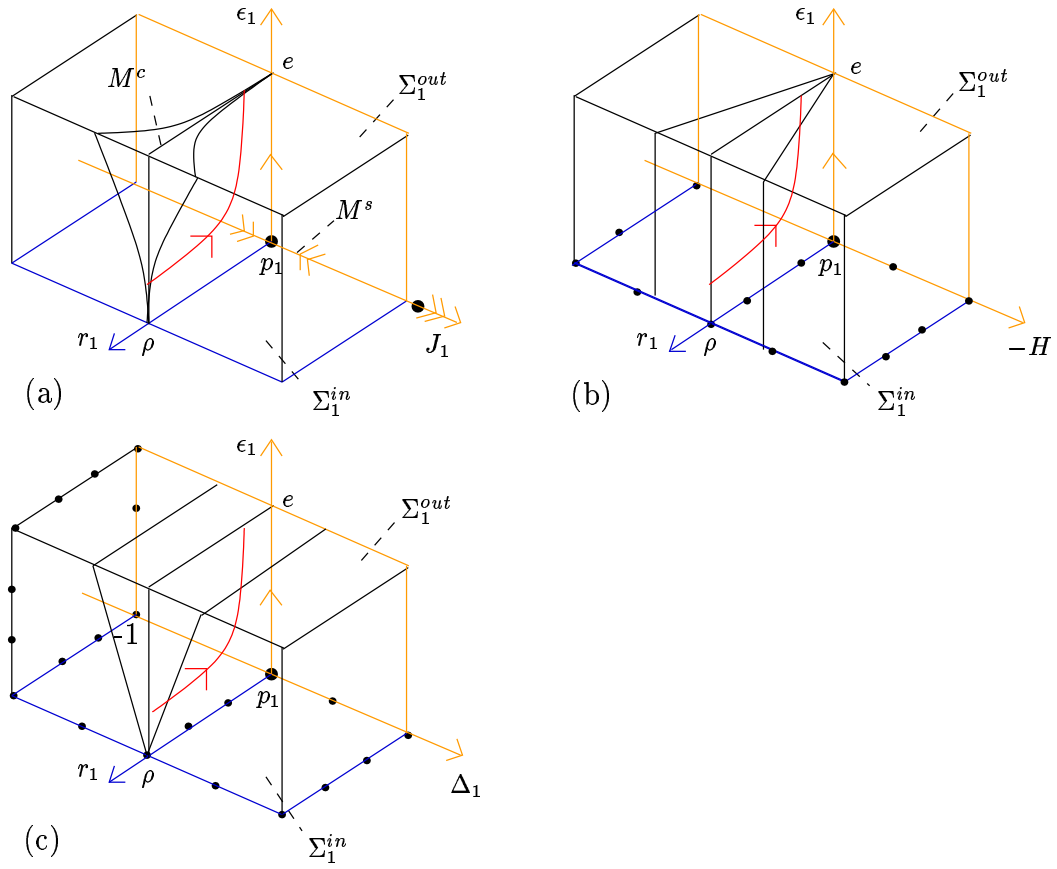

FIG. 4.11. *Dynamics in chart K_1*

corresponds to the manifold of equilibria N_2^s in chart K_2. There exists a third manifold of equilibria,

$$l_1^i := \{J_1 = \frac{1}{2((a-1)H)-1}, r_1 = 0, H, \varepsilon_1 = 0, \Delta_1 = 0\},$$

corresponding to l_3^i in chart K_3 which lies on the invariant 'sphere' $\{r_1 = 0\}$. These equilibria correspond to 'entrance points' to the sphere (and will not be important for us).

It is sufficient to describe the behaviour in a small neighborhood of $\{J_1 = 0\}$, so we calculate the invariant manifolds of the equilibrium $(J_1, r_1, H, \varepsilon_1, \Delta_1) = (0, 0, B, 0, 0)$:

Theorem 8. *At $p_1 := (0, 0, B, 0, 0)$ system (4.13) has a one-dimensional stable manifold M^s corresponding to the eigenvalue -1 tangent to $(1, 0, 0, 0, 0)^T$ and a 4-dimensional center manifold M^c corresponding to the eigenvalue 0 defined by $\{J_1 = 0\}$ in a small neighborhood of p_1 (see Fig.4.11(a)). There is a $c_1 > 0$, with c_1 close to 1 such that orbits near $\{J_1 = 0\}$ are attracted to $\{J_1 = 0\}$ by an exponential rate of order $O(e^{-c_1 t})$.*

Proof: Because $\{J_1 = 0\}$ is invariant and tangent to the center directions, it is a center manifold. The rest follows from standard center manifold theory [3]. □

For sufficiently small constants ρ, e the two sections Σ_1^{in} and Σ_1^{out} intersect the center manifold M^c of Theorem 8 transversally. Since $r_1\varepsilon_1 = \varepsilon$ and $r_1\Delta_1 = \Delta$ are constant we see that all orbits which start in Σ_1^{in} with $\varepsilon_{1i} > 0$ will exit in Σ_1^{out} with $r_{1o} = \varepsilon_{1i}\frac{\rho}{e}$ and $\Delta_{1o} = \Delta_{1i}\frac{\rho}{r_{1o}}$.

Lemma 9. *The leading term of the transition time T from Σ_1^{in} to Σ_1^{out} for orbits which start with $\varepsilon_{1i} \neq 0$ is of order $T \sim \varepsilon_{1i}^{-1}$.*

Proof: Since $\Delta_1 = \frac{\Delta_{1i}}{\varepsilon_{1i}}\varepsilon_1$ and $J_1 = 0$ the equation for ε_1 becomes

$$\varepsilon_1' = \varepsilon_1^2(\frac{\Delta_{1i}}{\varepsilon_{1i}}\varepsilon_1 + 1).$$

Integrating this equation for $-1 < \frac{\Delta_{1i}}{\varepsilon_{1i}}\varepsilon_1 < 0$ from $t = 0$ to $t = T$ gives

$$T = \{-\varepsilon_1^{-1} - \frac{\Delta_{1i}}{\varepsilon_{1i}} ln(\varepsilon_1) + ln(\frac{\Delta_{1i}}{\varepsilon_{1i}}\varepsilon + 1)\frac{\Delta_{1i}}{\varepsilon_{1i}}\} \mid_{\varepsilon_{1i}}^{e}$$

Because $\Delta_{1i} = O(\varepsilon_{1i})$ as we will see later, the dominating term in T is ε_{1i}^{-1}. □

From this we get estimates for the contraction of orbits which start in Σ_1^{in} near $J_1 = 0$:
Lemma 10. *Orbits which start with $J_{1i} = O(\varepsilon_{1i}^3)$ in section Σ_1^{in} will be attracted to $J_1 = 0$ exponentially: $J_{1o} = J_{1i}O(e^{-c_1/\varepsilon_{1i}})$.*
Proof: If $J_{1i} = O(\varepsilon_{1i}^3)$ and H and r_1 smaller than a constant, the additional terms for $J_1 \neq 0$ are only perturbations of higher order when integrating the ε_1' equation. The rest follows from Lemma 9 and Theorem 8. □

On the center manifold M^c the dynamics happens on the slower time scale t_1 and we get the following differential equation after dividing the right side by a common factor ε_1 for $\varepsilon_1 > 0$ (time transformation $\varepsilon_1 dt = dt_1$) in time t_1:

$$\begin{aligned} \dot{r}_1 &= -r_1(\Delta_1 + 1) \\ \dot{H} &= B + r_1\Delta_1 - H \\ \dot{\varepsilon}_1 &= \varepsilon_1(\Delta_1 + 1) \\ \dot{\Delta}_1 &= \Delta_1(\Delta_1 + 1). \end{aligned} \tag{4.14}$$

Because $\Delta = r_1\Delta_1 = r_{1i}\Delta_{1i}$ is constant we see that the dynamics in H is independent and can be integrated easily.
Lemma 11. *The transition time T_1 for equation (4.14) from Σ_1^{in} to Σ_1^{out} is of order $T_1 \sim -ln(\varepsilon_{1i})$.*
Proof: analogous to Lemma 9 for equation $\dot{\varepsilon}_1 = \varepsilon_1(\Delta_1 + 1)$ □

Since $H(t_1) = B + r_1\Delta_1 + (H_{1i} - (B + r_1\Delta_1))e^{-t_1}$ is the solution for H in the center manifold we get with Lemma 11:
Lemma 12. *In Σ_1^{out} H satisfies the relation $|H_{1o} - B| \sim |r_{1o}\Delta_{1o} + (H_{1i} - (B + r_{1o}\Delta_{1o}))\varepsilon_{1i}|$.*

The dynamics of the variables $r_1, \varepsilon_1, \Delta_1$ is independent of H. We see that the equations have an equilibrium in $(r_1, \varepsilon_1, \Delta_1) = (0, 0, 0)$ and the manifold of equilibria N_1^s for $\Delta_1 = -1$. For $\Delta_1 \neq -1$ we can again divide the right-hand side of equation (4.14) by $\Delta_1 + 1$ and get a linear system and therefore can draw the phase portrait. Here we see geometrically what happens to orbits which do not satisfy $-1 < \frac{\Delta_{1i}}{\varepsilon_{1i}}\varepsilon_1 < 0$. They will converge to an equilibrium in N_1^s for $\varepsilon_1 < e$. We are interested in orbits which exit at Σ_1^{out} with small $-1 < \Delta_{1o} < 0$ and therefore have to restrict our calculations to sufficiently small $\Delta_{1i} = O(\varepsilon_{1i})$.
Proposition 5. *If $J_{1i} = O(\varepsilon_{1i}^3)$, $-\frac{\varepsilon_{1i}}{2e} < \Delta_{1i} < 0$ there exist constants $c, \tilde{c}$ such that the map from Σ_1^{in} to Σ_1^{out} satisfies the following relations:*

1. *A wedge of size $|J_{1i}| \leq O(\varepsilon_{1i}^3)$ is mapped to a wedge of size $|J_{1o}| \leq O(e^{-c/r_{1o}})$.*
2. *The wedge $-\frac{\varepsilon_{1i}}{2e} < \Delta_{1i} \leq 0$ is mapped to the domain $-\frac{1}{2} < \Delta_{1o} \leq 0$.*
3. *A domain with $|H_{1i} - B| < \tilde{c}_1$ is mapped to a wedge of size $|H_{1o} - B| \leq \tilde{c}_2 r_{1o}$.*

Proof: Follows directly from the previous Lemmas with $r_{1o} = \varepsilon_{1i}\frac{\delta}{e}$, $\Delta = r_{1o}\Delta_{1o}$. □

Since $\gamma_1(\varepsilon_1, \Delta_1)$ satisfies the assumptions of Proposition 5 we get the following Theorem for γ_1 in Σ_1^{out}:
Theorem 9. *The manifold $\gamma_1(\varepsilon_1, \Delta_1)$ satisfies the following estimates in Σ_1^{out}:*

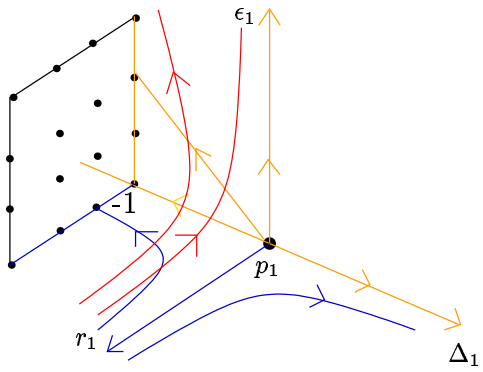

FIG. 4.12. *Dynamics in chart K_1 for r_1, ε_1 and Δ_1*

1. $|J_{1o}| \leq O(e^{-c/r_{1o}})$,
2. $-\frac{1}{2} < \Delta_{1o} \leq 0$, *and*
3. $|H_{1o} - B| \leq \tilde{c}_2 r_{1o}$.

4.6. Return to chart K_2. The change of coordinates from chart K_1 to chart K_2 in the overlap domain of K_1 and K_2, which is a diffeomorphism from $\{\varepsilon_1 > 0, r_1 > 0\}$ to $\{D_2 < 0, r_2 > 0\}$, is given by

$$J_2 = \varepsilon_1^{-2} J_1, \; D_2 = -\varepsilon_1^{-1}, \; r_2 = r_1 \varepsilon_1, \; \Delta_2 = \varepsilon_1^{-1} \Delta_1.$$

The out-section in chart K_1, Σ_1^{out}, is mapped to the in-section of chart K_2, Σ_2^{in}, defined by

$$\Sigma_2^{in} := \{D_{2i} = -e^{-1}, r_2 \in [0, \rho e]\}.$$

In chart K_2 the manifold $\gamma_1(\varepsilon_1, \Delta_1)$ is described by $\gamma_2(r_2, \Delta_2)$:

Lemma 13. *For sufficiently small r_{2i}, Δ_{2i} the manifold $\gamma_2(r_{2i}, \Delta_{2i})$ satisfies the following bounds in Σ_2^{in}:*

1. $|J_{2i}| \leq O(e^{-c/r_{2i}})$,
2. $|H_{2i} - B| \leq \frac{\tilde{c}_2}{e} r_{2i}$.

Proof: By combining the change of coordinates from K_1 to K_2 with Theorem 9. □

Next we will look how the manifold γ_2 evolves under the flow and describe its intersection with Ξ^{in}.

Proposition 6. *In Ξ^{in} the following bounds for $\gamma_2(r_2, \Delta_2)$ are satisfied(see Fig. 4.5 (a)):*

$$0 \leq J_2(r_{2i}, \Delta_{2i}) \leq O(e^{-c/r_{2i}})$$

$$|H(r_{2i}, \Delta_{2i}) - B| \leq K_2 r_{2i} \alpha e + r_{2i} \Delta_{2i} + O(e^{-c/r_{2i}}).$$

Proof: Because $D_2 \in [-\frac{1}{e}, -\alpha]$ and $J_2 > 0$, $J_2' = D_2 J_2 < 0$ and therefore $J_2 < J_{2i} = O(e^{-c/r_{2i}})$. Let $H \in [B-\beta, B+\beta]$ be an interval around B with $\beta > 0$ sufficiently small and $H_{2i} \in [B - \frac{\beta}{2}, B + \frac{\beta}{2}]$. Then H satisfies

$$H' = B + r_{2i}\Delta_{2i} - H + O(e^{-c/r_{2i}})$$

as long as it stays in the small interval.

$$H(t) = B + r_{2i}\Delta_{2i} + (H_{2i} - B - r_{2i}\Delta_{2i})e^{-t} + tO(e^{-c/r_{2i}})$$

is the solution for $t \in [0, T]$ with $T < \infty$. We see that for

$$|H(t, r_{2i}, \Delta_{2i}) - B| \leq (H_{2i} - B - r_{2i}\Delta_{2i})e^{-t} + r_{2i}\Delta_{2i} + tO(e^{-c/r_{2i}})$$

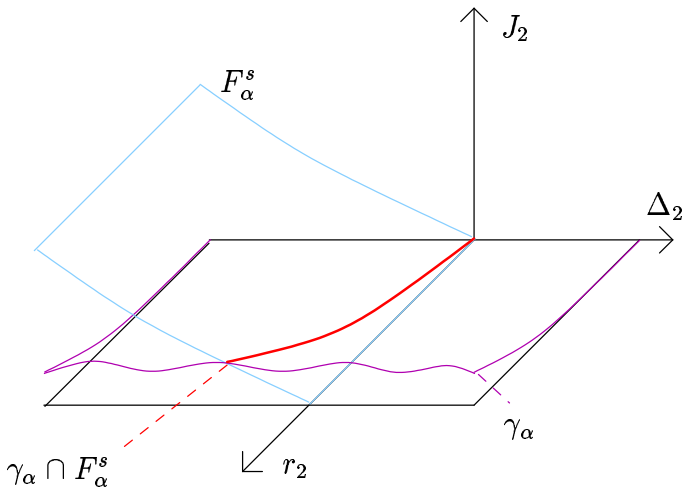

FIG. 4.13. *Intersection of F^s and $\gamma_2(r_2, \Delta_2)$ in Ξ^{in}*

the first term is smaller than $\frac{\beta}{2}$ and decreases for increasing t, $tO(e^{-c/r_{2i}}) = O(e^{-c/r_{2i}}) < \frac{\beta}{4}$ and $|r_{2i}\Delta_{2i}| < \frac{\beta}{4}$ for small r_{2i}. Therefore we can find for each T an upper bound for r_{2i} such that H remains in the interval. For $D_2 \in [-\frac{1}{e}, -\alpha]$ and $-\alpha < \Delta_2$, D_2 satisfies

$$D_2' = \Delta_2 - D_2 + O(e^{-c/r_{2i}}).$$

The solution is

$$D_2(t) = \Delta_2 + (-e^{-1} - \Delta_2)e^{-t} + O(e^{-c/r_{2i}})$$

for $t \in [0, T]$, $D_2 \leq -\alpha$ and $D_{2i} = -e^{-1}$. The equation

$$D_2(T_\alpha) = -\alpha$$

has the solution

$$e^{-T_\alpha} = \frac{\alpha + \Delta_2}{e^{-1} + \Delta_2} + O(e^{-c/r_{2i}}).$$

With $|H_i - B - r_{2i}\Delta_{2i}| < K_2 r_{2i}$ and $|\frac{\alpha+\Delta_2}{e^{-1}+\Delta_2}| < \alpha e$ we get the bounds for $|H(r_{2i}, \Delta_{2i}) - B|$. □

Now that we know the intersection M^s_α of the stable manifold M^s, which is equal to the stable foliation F^s over N^u_2, with Ξ^{in} and the intersection γ_α of the returning flow $\gamma(r_2, \Delta_2)$ with Ξ^{in} we can describe the intersection of M^s and $\gamma(r_2, \Delta_2)$ in Ξ^{in}. Because Ξ^{in} is transversal to γ_2 and F^s it is sufficient to look for which parameter values this intersection occurs in Ξ^{in}.

Theorem 10. *The intersection of $\gamma(r_2, \Delta_2)$ and M^s (see Fig. 4.13) exists for*

$$\Delta_2 = \Delta_2(r_2) = O(e^{-c/r_2}).$$

Proof: From Theorem 2 and Proposition 6 we obtain equations for the intersection of the manifolds:

$$\begin{pmatrix} \delta_n(\frac{-1}{aB-B-1} + \overline{f}_1(-\alpha + O(\delta_n), h_n, r_n, \delta_n)) \\ -\alpha \\ B + h_n \\ r_n \\ \delta_n \end{pmatrix} = \begin{pmatrix} J_2(r_2, \Delta_2) \\ -\alpha \\ H(r_2, \Delta_2) \\ r_2 \\ \Delta_2 \end{pmatrix}$$

with $J_2(r_2,\Delta_2)=O(e^{-c/r_2})$ and $H(r_2,\Delta_2)=B+O(r_2)$. This leads to the equations

$$0=g_1=\Delta_2(\frac{-1}{aB-B-1}+\overline{f}_1(-\alpha+O(\Delta_2),h_n,r_2,\Delta_2))+O(e^{-c/r_2})$$
$$0=g_2=h_n+O(r_2).$$

In $\Delta_2=r_2=h_n=0$ the Jacobian

$$\frac{\partial(g_1,g_2)}{\partial(\Delta_2,h_n)}=\begin{pmatrix}(\frac{-1}{aB-B-1}+\overline{f}_1(-\alpha,0,0,0))) & 0\\ 0 & 1\end{pmatrix}$$

is regular if α is sufficiently small. By the Implicit Function Theorem the equations can be solved for Δ_2 and h_n which gives:

$$\Delta_2=\Delta_2(r_2,B,a,\alpha)=O(e^{-c/r_2})$$
$$h_n=h_n((r_2,B,a,\alpha))=O(r_2).$$

Because Δ_2 is independent of α we get $\Delta_2=\Delta_2(r_2,B,a)=O(e^{-c/r_2})$. □

This can be easily understood geometrically. For the stable foliation M^s_α the manifold

$$J_2(r_2,\Delta_2)=\Delta_2(\frac{-1}{aB-B-1}+\overline{f}_1(-\alpha+O(\Delta_2),h_n,r_2,\Delta_2))$$

is transversal to $\{J_2=0\}$ because $|\overline{f}_1|<\frac{1}{aB-B-1}$ for α,h_n,r_2,Δ_2 sufficiently small. On the other side γ_α satisfies

$$J_2(r_2,\Delta_2)=O(e^{-c/r_2})$$

for the returning manifold and is tangent to $\{J_2=0\}$ in $\{r_2=0\}$ (see Fig.4.5). Therefore the two manifolds intersect transversally (see Fig. 4.13) along $\Delta_2=O(e^{-c/r_2})$ and the orbits of the manifold $\gamma_2(r_2,\Delta_2)$ tend to N^u_s for these parameter values.

4.7. Summary of the proof of Theorem 1. Here we collect the results we have established in the various charts. An overview over the different sections Ξ and Σ we have used is given in Fig. 4.14. We describe the evolution of the 2-dimensional manifold $\gamma(\varepsilon,\Delta)$ attached to the singular orbit $\gamma(0,0)$ which contains the homoclinic orbits $\gamma(\varepsilon,\Delta_{Hom})$ as a submanifold.

In chart K_2 the manifold $\gamma_2(\varepsilon_2,\Delta_2)$ starts as the invariant unstable C^k manifold M^u of N^u_2. Its intersection with Ξ^{out} is given in Theorem 3.

In chart K_3 the transition from Σ^{in}_3 to Σ^{out}_3 is described in two steps. The transition from Σ^{in}_3 to Σ^e_3 is a diffeomorphism. The intersection $\gamma_3\cap\Sigma^e_3$ is still C^k (Lemma 5). During the transition from Σ^e_3 to Σ^{out}_3 it looses some of its smoothness. This is due to resonances of the non-hyperbolic equilibrium p^o_3. This transition is described in Theorem 5 by transformation to Fenichel coordinates and Gronwall-like estimates to get bounds on the variables and derivatives of $\gamma_3\cap\Sigma^{out}_3$. The bounds on the derivatives are of order $O(ln(\varepsilon_3))$.

Then the transition from Σ^{out}_3 to Σ^{in} is described in original coordinates as a regular perturbation of the layer problem (Theorem 6).

The transition from Σ^{in} to Σ^{out} is described by the Fenichel theory in Theorem 7. Due to the attraction of $\gamma(\varepsilon,\Delta)$ to $J=0$ by an exponential rate of order $O(e^{-c/\varepsilon})$ the J component of $\gamma(\varepsilon,\Delta)$ regains differentiability: the derivatives of $J=O(e^{-c/\varepsilon})$ can be continuously extended to $\varepsilon=0$.

In chart K_1 the transition from Σ^{in}_1 to Σ^{out}_1 is described with the center manifold in p and its foliation (Theorem 8). The intersection $\gamma_1\cap\Sigma^{out}_1$ is described in Theorem 9. Due to the relation $|H_{1o}-B|\sim|r_{1o}\Delta_{1o}+(H_{1i}-B)\varepsilon_{1i}|$ (Lemma 11) the derivatives of the variable H_{1o} of $\gamma_1\cap\Sigma^{out}_1$ are continuously extendable, too. Therefore the manifold $\gamma_1\cap\Sigma^{out}_1$ is a C^1 manifold.

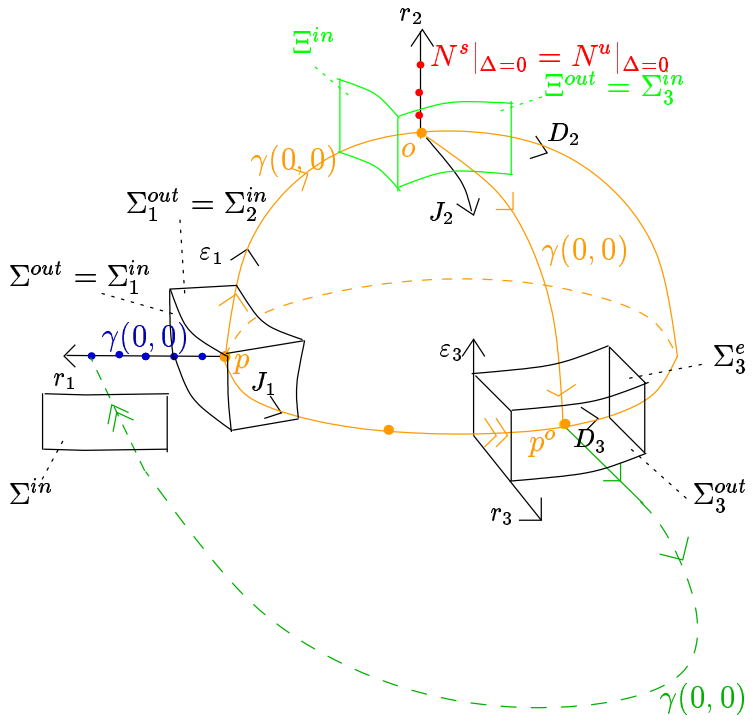

FIG. 4.14. *The different sections Σ transversal to the homoclinic orbit γ of the proof*

Next we describe the transition from $\Sigma_2^{in} = \Sigma_1^{out}$ to Ξ^{in} which is a diffeomorphism (Proposition 6). A transcritical bifurcation of the curves N_2^s and N_2^u which takes place in the 3-dimensional center manifold in q_2 (Lemma 3, Lemma 4). A homoclinic orbits exists for the parameter values of ε_2, Δ_2 where the orbit $\gamma_2(\varepsilon_2, \Delta_2)$ converges to an equilibrium in N_2^u. This means that $\gamma_2(\varepsilon_2, \Delta_2)$ intersects the stable manifold M^s of N_2^u. In Theorem 10 we have shown that this intersection is transversal and takes place for a unique curve of parameters $\Delta_2 = \Delta_2(r_2) = O(e^{-c/r_2})$. Because $\varepsilon = r_2$ and $\Delta = r_2\Delta_2$ this completes the proof of Theorem 1. □

Appendix A. Proof of Theorem 4. The center-stable manifold M^{cs} and the center manifold M^c in p_3^o of system (4.11) are flat already, $M^{cu} \subseteq \{r_d = 0\}$ and $M^c \subseteq \{r_d = d_d = \varepsilon_d = \Delta_d = 0\}$. The center-unstable manifold M^{cu} is tangent to $E^{cu} = \{d_d = \varepsilon_d = \Delta_d = 0\}$ in p_3^o. According to center manifold theory it can be described by C^k functions ψ_i of order $O(\|(r_d, h_d)\|^2)$:

$$d_d = \psi_1(r_d, h_d),\ \varepsilon_d = \psi_2(r_d, h_d),\ \Delta_d = \psi_3(r_d, h_d).$$

Because of the simple form of system (4.11), we have $\psi_2 \equiv 0$ and $\psi_3 \equiv 0$. Because $M^{cu}|_{r_d=0} \subseteq M^c$ we get $d_d = \psi_1(0, h_d) = 0$ and there exists some $\tilde{\psi}_1$ such that

$$d_d = r_d\tilde{\psi}_1(r_d, h_d),\ \varepsilon_d = 0\ \Delta_d = 0.$$

We change to the new coordinates $\tilde{d}$ defined by $d_d = r_d\tilde{\psi}_1(r_d, h_d) + \tilde{d}$ where $\tilde{d} = r_d = \varepsilon_d = 0$ corresponds to M^{cu}. In this system we have

$$\tilde{d}' = d' - r'\tilde{\psi}_1 - r\tilde{\psi}_{1r}r' - r\tilde{\psi}_{1h} = -\tilde{d} + O(\|(..)\|^2)$$

again.

Next we straighten the fibers in the center-stable manifold $M^{cs} \subseteq \{r_d = 0\}$. The fibers can be described by

$$\begin{pmatrix} \tilde{d} \\ h_d \\ \varepsilon_d \\ \Delta_d \end{pmatrix} = \begin{pmatrix} 0 \\ h_c \\ 0 \\ 0 \end{pmatrix} + \begin{pmatrix} d_s \\ f(h_c, d_s, \varepsilon_s, \Delta_s) \\ \varepsilon_s \\ \Delta_s \end{pmatrix}$$

with a C^{k-1} function f. The center manifold is characterized by $d_s = \varepsilon_s = \Delta_s = 0$ and $f(h_c, 0, 0, 0) = 0$. The fiber of p_3^o is described by $h_c = 0$ because p_3^o is part of the invariant submanifold $\{h_d = 0, r_d = 0\}$. Therefore $f(0, d_s, \varepsilon_s, \Delta_s) = 0$ and there exists a function F such that

$$\begin{pmatrix} \tilde{d} \\ h_d \\ \varepsilon_d \\ \Delta_d \end{pmatrix} = \begin{pmatrix} 0 \\ h_c \\ 0 \\ 0 \end{pmatrix} + \begin{pmatrix} d_s \\ h_c(d_s, \varepsilon_s, \Delta_s)^T F(h_c, d_s, \varepsilon_s, \Delta_s) \\ \varepsilon_s \\ \Delta_s \end{pmatrix}.$$

Next we define a map P by

$$P(\tilde{d}, h_d, \varepsilon_d, \Delta_d) := h_c,$$

which maps each point of a fiber to its intersection with M^c. We obtain this map by solving

$$h_d = h_c + h_c(d_s, \varepsilon_s, \Delta_s)^T F(h_c, d_s, \varepsilon_s, \Delta_s)$$

for h_c corresponding to the Implicit Function Theorem which gives

$$h_c = P(d_d, h_d, \varepsilon_d, \Delta_d) = h_d + h_d(d_s, \varepsilon_s, \Delta_s)^T \tilde{P}(h_d, d_s, \varepsilon_s, \Delta_s).$$

Next we change to the new variable

$$\tilde{h} := h_c = h_d + h_d(\tilde{d}, \varepsilon_d, \Delta_d)^T \tilde{P}(h_d, \tilde{d}, \varepsilon_d, \Delta_d),$$

which leaves M^{cu} invariant. In the new variables $(r_d, \tilde{d}, \tilde{h}, \varepsilon_d, \Delta_d)$ the fibers are flat in M^{cs}.

Following the analog steps to straighten out the fibres in $M^{cu} \subseteq \{d_d = \varepsilon_d = \Delta_d = 0\}$ gives the transformation to another new variable $\tilde{\tilde{h}}$:

$$\tilde{\tilde{h}} := \tilde{h} + \tilde{h} r_d \tilde{\tilde{P}}(r_d).$$

This transformation leaves M^{cs} invariant. In the new coordinates $r = r_d, d = \tilde{d}, h = \tilde{\tilde{h}}, \varepsilon = \varepsilon_d, \Delta = \Delta_d$ we get a system of the form (4.10):

$$\begin{aligned} r' &= \frac{1}{2} r \\ d' &= -d + f_2(r, d, h, \varepsilon, \Delta) \\ h' &= f_3(r, d, h, \varepsilon, \Delta) \\ \varepsilon' &= -\frac{1}{2}\varepsilon \\ \Delta' &= -\frac{1}{2}\Delta, \end{aligned} \tag{A.1}$$

with f_2, f_3 C^{k-1} functions of order $O(\|(..)\|^2)$. Due to the above transformations we know: $f_2 = 0$ for $d = \varepsilon = \Delta = 0$, which means that $f_2 = \Lambda(r, d, h, \varepsilon, \Delta)(d, \varepsilon, \Delta)^T$, f_3 is independent of $r, d, \varepsilon, \Delta$ for $d = \varepsilon = \Delta = 0$ or $r = 0$, which means $f_3 = f_3(0, 0, h, 0, 0) + H(r, d, h, \varepsilon, \Delta)(d, \varepsilon, \Delta)^T r$. Because M^c is a line of equilibria we have $f_3(0, 0, h, 0, 0) \equiv 0$.

Applying the change of coordinates to our initial conditions does not change their form compared to Lemma 7.

Appendix B. Proof of Proposition 4. The proof of Proposition 4 is technical and is split into several lemmas and propositions. We will describe the transition by first integrating the equations for $r = 0$ from 0 to the transition time T and calculating some bounds for the solution $d(t)$ with $r = 0$. Afterwards we use this result to calculate bounds for $d(t)$ and $h(t)$ for $r > 0$. As a last step we derive bounds for the derivatives of $d(t)$, $h(t)$ with respect to Δ_i, r_i. For the transition time T we have:

$$T = 2ln(\frac{\rho}{r_i}).$$

First we will look at system (4.12) for $r = 0$ and $d = d_i, h = h_i, \varepsilon = \varepsilon_i, \Delta = \Delta_i$:

$$\begin{aligned} d' &= -d + \Lambda_0(d, h, \varepsilon, \Delta)(d, \varepsilon, \Delta)^T \\ h' &= 0 \\ \varepsilon' &= -\frac{1}{2}\varepsilon \\ \Delta' &= -\frac{1}{2}\Delta, \end{aligned} \tag{B.1}$$

where h is a constant. When we apply the transformation to normal form we get:

Lemma 14. *In normal form coordinates of order $O(p)$ the equation for d' is:*

$$d' = -d + dg_1(h) + \varepsilon^2 g_2(h) + \varepsilon\Delta g_3(h) + \Delta^2 g_4(h) + O(p),$$

where g_1 is a polynomial of order 1 in h and the other g_i are of order 0 in h. The term $O(p)$ consists of functions of order $O(\|(d, h, \varepsilon, \Delta)\|^p)$ (which have Fenichel form).

Proof: It is easy to see that the only resonant terms are dh^{k+1}, $\varepsilon^2 h^k$, $\varepsilon\Delta h^k$, $\Delta^2 h^k$ with $k \geq 0$. The normal form transformation is of the form $d = \bar{d} + \psi(\bar{d}, h, \varepsilon, \Delta)$ with $\psi = O(\|(\bar{d}, \varepsilon, \Delta)\|)O(\|(\bar{d}, h, \varepsilon, \Delta)\|)$. This and the special form of the equations for the other variables lead to a new equation for $\bar{d}$ which again has Fenichel form. (We omit the $^-$ in the following.) □

We can solve the system (B.1) for the variables

$$\varepsilon = \varepsilon_i e^{-t/2}, \ \Delta = \Delta_i e^{-t/2}$$

explicitly. Next we make the assumption that all solutions for $t \in [0, T]$ lie in a small region

$$U := \{r, d, h, \Delta \in [-\rho, \rho], \ \varepsilon \in [0, e]\}.$$

We will show later (at the end of Lemma 17) that this is satisfied if the initial conditions are chosen appropriately and ρ, e are sufficiently small. First we compute bounds for higher order terms. As notation, we use C_i for bounds which are simple constants and K_i for bounds for terms of order $O(\|(\bar{d}, d, h, \varepsilon, \Delta, \varepsilon_i, \Delta_i)\|)$, which means $K_i = O(\|(\rho, e)\|)$. We use the Fenichel form of the higher order terms $O(p)$ to get:

Lemma 15. *The solution $d(t)$ of system (B.1) is a solution of an equation of the form*

$$d' = -d + df_1(d, h, \varepsilon, \Delta) + e^{-t} f_2(d, h, \varepsilon, \Delta, \varepsilon_i, \Delta_i) + e^{-1/2t} h^{p-1} f_3(d, h, \varepsilon, \Delta, \varepsilon_i, \Delta_i)$$

with $\|f_1\| \leq K_1$, $\|f_2\| \leq K_2$, $\|f_3\| \leq K_3$ on U with the initial condition $d(0) = d_i$.

Proof: For the equation in Lemma 14 we can separate the resonant and non-resonant terms in two different groups:

- terms of order $O(\|d\|)$, which are

$$dg_1(h), \ dO(\|(d, h, \varepsilon, \Delta)\|^{p-1})$$

- terms of order $O(\|d\|^0)$, which are

$$\varepsilon^2 g_2(h),\ \varepsilon\Delta g_3(h),\ \Delta^2 g_4(h),\ O(\|(\varepsilon,\Delta)\|^2)O(\|(h,\varepsilon,\Delta)\|^{p-2}),\ O(\|(\varepsilon,\Delta)\|)|h|^{p-1}.$$

The first kind can be described by $df_1(d,h,\varepsilon,\Delta)$ with $f_1 = O(\|(d,h,\varepsilon,\Delta)\|)$. If we plug the solutions $\varepsilon(t)$ and $\Delta(t)$ in the second kind of terms we can collect the first four terms to $e^{-t}f_2(d,h,\varepsilon,\Delta,\varepsilon_i,\Delta_i)$ with $f_2 = O(\|\varepsilon_i,\Delta_i)\|^2)$ and the last term has the form $e^{-1/2t}h^{p-1}f_3(d,h,\varepsilon,\Delta,\varepsilon_i,\Delta_i)$ with $f_3 = O(\|\varepsilon_i,\Delta_i)\|)$. Because the f_i are higher order terms there exists small constants K_i such that $f_i \leq K_i$ (which can be chosen smaller when ρ, e get smaller). □

We will use the following relation:

Lemma 16. *(Lemma of Gronwall) The assumptions $J := \{t \in [0,T]\}$, $g(t), v(t) \in C(J)$, $0 \leq h(t)$ Lebesgue integrable on J together with the inequality*

$$v(t) \leq g(t) + \int_0^t h(\tau)v(\tau)d\tau$$

imply

$$v(t) \leq g(t) + \int_0^t g(\tau)h(\tau)e^{H(t)-H(\tau)}d\tau$$

with $H(t) = \int_0^t h(\tau)d\tau$ (see [26] p.15).

With these Lemmas we get:

Lemma 17. *The solution to the equation of Lemma 15 has the form*

$$d(t) = (d_0(t) + d_1(t)t + d_2(t)t^2)e^{-t} + h^{p-1}d_3(t)e^{-t/2}$$

where $|d_0(t)| \leq |d_i|$, $|d_1(t)| \leq |d_i|K_1e^{K_1} + K_2$, $|d_2(t)| \leq K_2K_1e^{K_1}$ and $|d_3(t)| \leq 2K_3(1 + K_1e^{K_1})$ for $t \in [0,T]$.

Proof: We first transform the equation of Lemma 15 to the equivalent integral equation and then take the absolute value. So we get

$$|d| \leq e^{-t}|d_i| + \int_0^t e^{-t+\tau}|df_1 + e^{-\tau}f_2 + e^{-\tau/2}h^{p-1}f_3|d\tau.$$

Taking into account the bounds on the f_i we get the inequality

$$|d| \leq e^{-t}|d_i| + \int_0^t e^{-t}(K_2 + e^{\tau/2}|h|^{p-1}K_3)d\tau + \int_0^t e^{-t}K_1|d|d\tau.$$

The terms in the Gronwall inequality are
$g(t) = (|d_i| + K_2t)e^{-t} + K_3|h|^{p-1}2(e^{-t/2} - e^{-t})$ and
$H(t) - H(\tau) = K_1(e^{-\tau} - e^{-t}) \leq K_1$. Plugging these terms into the Gronwall inequality and integration yields

$$|d| \leq (|d_i| + K_2t + (|d_i|t + K_2t^2/2)K_1e^{K_1})e^{-t} + K_3|h|^{p-1}2(e^{-t/2} - e^{-t} + 2(e^{-t/2} - e^{-t} - te^{-t})K_1e^{K_1})$$

$$\leq |d_i| + |d_i|K_1e^{K_1} + K_2 + K_2K_1e^{K_1} + 2K_3(1 + K_1e^{K_1})$$

(because of $e^{-t} \leq 1, te^{-t} \leq 1, t^2e^{-t} \leq 1$ for $t \geq 0$) which leads to the assertion of the Lemma if we can verify that $d(t)$ indeed satisfies our assumption $d(t) \in [-\rho,\rho]$. We define

$$V := \{(d_i,\varepsilon_i,\Delta_i)|d_i,\Delta_i,\varepsilon_i \in [-\beta,\beta]\}$$

where β is a small positive constant such that $\beta \leq e,\rho$. We define the constants $K_2 := sup_{U,|\varepsilon_i|\leq\beta,|\Delta_i|\leq\beta}f_2(d,h,\varepsilon,\Delta,\varepsilon_i,\Delta_i)$ and analogously K_3 which means $K_2 = O(\beta^2)$, $K_3 = O(\beta)$. We can choose β sufficiently small such that

$$|d_i| + |d_i|K_1e^{K_1} + K_2 + K_2K_1e^{K_1} + 2K_3(1 + K_1e^{K_1}) < \rho$$

is satisfied.

Suppose that under the above conditions there exists a $t^* < T$ such that $|d(t)| < \rho$ for $t \in [0, t^*)$ and $|d(t^*)| = \rho$. Then we can perform the proof of this Lemma for $t \in [0, t^*]$ which leads to the contradiction $|d(t^*)| < \rho$. This means that the assumptions are valid for $t \in [0, T]$ and the statement of the Lemma follows. □

As a next step we will calculate the solution for the equation for $r > 0$.

Lemma 18. *For $r > 0$ system (4.12) is equivalent to*

$$\begin{aligned} r' &= \frac{1}{2}r \\ d' &= -d + \Lambda_N(d, h, \varepsilon, \Delta)(d, \varepsilon, \Delta)^T + r\Lambda_1(r, d, h, \varepsilon, \Delta)(d, \varepsilon, \Delta)^T \\ h' &= H(r, d, h, \varepsilon, \Delta)(d, \varepsilon, \Delta)^T r \\ \varepsilon' &= -\frac{1}{2}\varepsilon \\ \Delta' &= -\frac{1}{2}\Delta, \end{aligned} \tag{B.2}$$

where Λ_N is the nonlinear part of Lemma (14) and Λ_1 of order $O(1)$. The initial conditions have the form $h_i = r_i h^*(r_i, \Delta_i)$, $d = d_i^*(r_i, \Delta_i)$.

Proof: In equation (4.12) Λ_1 would be of order $O(0)$. Because all terms $rd, r\varepsilon, r\Delta$ are not resonant we can apply one step of normal form transformation and get a new system where Λ_1 is of order $O(1)$. Further the Fenichel form and the special form of the initial conditions will be preserved. □

If we plug the solutions for $r(t), d(t), \Delta(t)$ into equation (B.2) we get a 2-dimensional system for d' and h'. Because it is easier to apply the Lemma of Gronwall to 1-dimensional systems, we make the assumption that

$$h(t) = h_i + r_i t h_1(t) \tag{B.3}$$

with $|h_1| \leq C$. For $d(t)$ we make the Ansatz

$$d(t) = \bar{d}(t) + r_i d_4(t), \tag{B.4}$$

where $\bar{d}(t)$ is the solution for $r = 0$. Further we make the assumptions $|d_4| \leq C$, $|h| \leq \rho$ on $[0, T]$. (The validity of these assumptions is shown at the end of the proof of Proposition 7.)

Lemma 19. *$d_4(t)$ is a solution to the equation*

$$d_4' = -d_4 + d_4 f_1 + g_f + r_i d_4 g_1$$

with $f_1 = f_1(\bar{d}, h, \varepsilon, \Delta, r_i d_4) \leq L_0$, $g_f = g_f(\bar{d}, h, \varepsilon, \Delta, r) \leq K_L$ and $g_1 = g_1(\bar{d}, h, \varepsilon, \Delta, r, r_i d_4) \leq L_1 e^{t/2}$ with the three small constants L_0, L_1, K_L.

Proof: We define $f := \Lambda_N(d, \varepsilon, \Delta)^T$ and $g := e^{t/2}\Lambda_1(d, \varepsilon, \Delta)^T$. Because $|f_d| = |\Lambda_{Nd}(d, \varepsilon, \Delta)^T + \Lambda_N(1, 0, 0)^T| = O(1)$ and $|g_d| = |e^{t/2}\Lambda_{1d}(d, \varepsilon, \Delta)^T + e^{t/2}\Lambda_1(1, 0, 0)^T| = e^{t/2}O(1)$ we get the two small Lipschitz constants $|f_d| \leq L_0$, $|g_d| \leq L_1 e^{t/2}$ on U small enough. From the Mean Value Theorem we have that there exists some $\vartheta \in (0, s)$ such that

$$\frac{f(d + s, h, \varepsilon, \Delta) - f(d, h, \varepsilon, \Delta)}{s} = f_d(d + \vartheta, h, \varepsilon, \Delta) =: f_1(d, h, \varepsilon, \Delta, s)$$

with $|f_1| \leq L_0$ and analogously

$$\frac{g(d + s, h, \varepsilon, \Delta, r) - g(d, h, \varepsilon, \Delta, r)}{s} = g_d(d + \vartheta, h, \varepsilon, \Delta, r) =: g_1(d, h, \varepsilon, \Delta, r, s)$$

with $|g_1| \leq L_1 e^{t/2}$. Further we have that because

$$(\bar{d}, \varepsilon, \Delta)^T = e^{-t/2}((d_0 + t d_1 + t^2 d_2)e^{-t/2} + h_i^{p-1} d_3, \varepsilon_i, \Delta_i)^T$$

and $\Lambda_1 = O(1)$ there exists some small constant K such that

$$|g(\bar{d}, h, \varepsilon, \Delta, r)| = |e^{t/2}\Lambda_1(\bar{d}, h, \varepsilon, \Delta, r)(\bar{d}, \varepsilon, \Delta)^T| \leq K.$$

Analogously we get for $h = h_i + r_i t h_1$ that

$$\frac{f(d, h, ...) - f(d, h + s, ...)}{s} =: f_2(d, h_i, ..., s)$$

with $|f_2| \leq L_2$. We use these relations on the equation

$$d' = -d + f(d, h, \varepsilon, \Delta) + r_i g(d, h, \varepsilon, \Delta, r)$$

and get

$$\begin{aligned}\bar{d}' + r_i d_4' &= -(\bar{d} + r_i d_4) + f(\bar{d} + r_i d_4, h_i + r_i t h_1, ...) + r_i g(\bar{d} + r_i d_4, ...) \\ &= -(\bar{d} + r_i d_4) + f(\bar{d}, h_i ...) + f_2(\bar{d}, h_i, ..., r_i t h_1) r_i t h_1 + r_i d_4 f_1(\bar{d}, h, ..., r_i d_4) + \\ &\quad + r_i g(\bar{d}, ...) + r_i^2 d_4 g_1(\bar{d}, ..., r_i d_4).\end{aligned}$$

$\bar{d}$ solves the equation $\bar{d}' = -\bar{d} + f(\bar{d}, h_i, ...)$, which we substract, and divide by r_i and so finally get the differential equation

$$d_4' = -d_4 + f_2 r_i t h_1 + d_4 f_1 + g + r_i d_4 g_1$$

Because $f_2 r_i t h_1 \leq L_2 e^{-t/2} t C \leq L_2 C$ and $|g| \leq K$ we can define a new function

$$g_f := f_2 r_i t h_1 + g, |g_f| \leq K_L.$$

□

Proposition 7. *The solution of system (B.2) has the form*

$$\begin{aligned} d(t) &= (d_0(t) + d_1(t)t + d_2(t)t^2)e^{-t} + h_i^p d_3 e^{-t/2} + r_i d_4(t) \\ h(t) &= h_i + r_i t h_1(t) \end{aligned} \tag{B.5}$$

with $t \in [0, T]$, $|d_4(t)| \leq K_L + 2K_L(L_0 + \rho L_1)e^{L_0 + \rho L_1}$ *and* $|h_1(t)| \leq K_3$.
Proof: With Lemma 19 we get the solution $d(t)$ by transforming to a integral equation and applying the Lemma of Gronwall analogously to Lemma 17. For h we plug the solution for d into equation (B.2). For $h' = H(d, \varepsilon, \Delta)r$ we get that $|H| \leq C$ and as above

$$\|(d, \varepsilon, \Delta)^T r\| = \|((d_0 + t d_1 + t^2 d_2)e^{-t/2} r_i + h_i^{p_1} d_3 r_i + r_i d_4 r_i e^{-t/2})\| \leq r_i K_4.$$

The integral equation for h leads to

$$|h| \leq |h_i + \int_0^t H(d, \varepsilon, \Delta)r| \leq h_i + \int_0^t C r_i K_4 = h_i + r_i t K_4$$

and we get $h(t) = h_i + r_i t h_1(t)$ with $|h_1| \leq K_4$.

Again we have to show that the assumptions for $h(t)$, $d(t)$ hold. If we choose U and V appropriately the constants K_L and K_4 get sufficiently small such that $|d_4| \leq K_L + 2K_L(L_0 + \rho L_1)e^{L_0 + \rho L_1} < C$, $|h_1| \leq K_4 < C$, $d(t) < \rho$, $h(t) < \rho$ and $|\bar{d}| \in \rho/2$, which is show analogously as in Lemma 17. □

For the transition map Π we need to show that $d_{\Delta_i}(T), h_{\Delta_i}(T), d_{r_i}(T), h_{r_i}(T)$ is sufficiently smooth. Therefore we look at the variational equations. If we write the equations as

$$\begin{aligned} d' &= -d + \tilde{D} = -d + (\Lambda_0 + r\Lambda_1)(d, \varepsilon, \Delta)^T \\ h' &= \tilde{H} = H(d, \varepsilon, \Delta)^T, \end{aligned}$$

we get the variational equations

$$d'_{\Delta_i} = -d_{\Delta_i} + \tilde{D}_{\Delta_i} = -d_{\Delta_i} + \tilde{D}_d d_{\Delta_i} + \tilde{D}_h h_{\Delta_i} + \tilde{D}_\Delta e^{-t/2}$$
$$h'_{\Delta_i} = \tilde{H}_{\Delta_i} = \tilde{H}_d d_{\Delta_i} + \tilde{H}_h h_{\Delta_i} + \tilde{H}_\Delta e^{-t/2}$$

and

$$d'_{r_i} = -d_{r_i} + \tilde{D}_{r_i} = -d_{r_i} + \tilde{D}_d d_{r_i} + \tilde{D}_h h_{r_i} + \tilde{D}_r e^{t/2}$$
$$h'_{r_i} = \tilde{H}_{r_i} = \tilde{H}_d d_{r_i} + \tilde{H}_h h_{r_i} + \tilde{H}_r e^{t/2}.$$

Because $\tilde{D}_d = (\Lambda_{0d} + r\Lambda_{1d})(d, \varepsilon, \Delta)^T + (\Lambda_0 + r\Lambda_1)(1, 0, 0)^T = O(1)$, similarly $\tilde{D}_\Delta = O(1)$ and with $\|(d, \varepsilon, \Delta)\| = \|((d_0 + td_1 + t^2 d_2)e^{-t/2} + h_i^{p-1} d_3 + r_i e^{t/2} d_4, \varepsilon_i, \Delta_i)\| e^{-t/2} \leq K_4 e^{-t/2}$, $\tilde{D}_h = O(1)e^{-t/2}$ and $\tilde{D}_r = O(1)e^{-t/2}$ we get the bounds:

$$|\tilde{D}_d| \leq K_5,\ |\tilde{D}_h| \leq K_6 e^{-t/2},\ |\tilde{D}_\Delta| \leq K_7,\ |\tilde{D}_r| \leq K_8 e^{-t/2}.$$

In a similar way, because $r = r_i e^{t/2}$, we get

$$|\tilde{H}_d| \leq C_1 r,\ |\tilde{H}_h| \leq K_9 r_i,\ |\tilde{H}_\Delta| \leq C_2 r,\ |\tilde{H}_r| \leq K_{10} r_i + K_{11} e^{-t/2}.$$

We again need some assumptions for h on $[0, T]$: there exists some C, $\alpha \in (0, 1)$ such that

$$|h_{\Delta_i}| \leq C,\ |r_i^\alpha h_{r_i}| \leq C.$$

Proposition 8. *With $|d_i(r_i, \Delta_i)_{\Delta_i}| \leq C_3$ and $|h_i(r_i, \Delta_i)_{\Delta_i}| \leq r_i C_4$ the derivatives satisfy*

$$|d_{\Delta_i}(t)| \leq e^{-t} C_3 + K_{13} t e^{-t} + K_{14}(e^{-t/2} - e^{-t})$$
$$|h_{\Delta_i}(t)| \leq r_i C_5 + C_6 r_i t$$

for some small constants K_{13}, K_{14} and constants C_5, C_6.
Proof: An equivalent integral equation for $d_{\Delta_i}(t)$ is

$$\begin{aligned} d_{\Delta_i} &= e^{-t} d_{i\Delta_i} + \int_0^t e^{-t+\tau} \tilde{D}_{\Delta_i} d\tau \\ &= e^{-t} d_{i\Delta_i} + \int_0^t e^{-t+\tau} (\tilde{D}_d d_{\Delta_i} + \tilde{D}_h h_{\Delta_i} + \tilde{D}_\Delta e^{-\tau/2}) d\tau. \end{aligned}$$

With the assumption $|h_{\Delta_i}| \leq C$ and the bounds on the derivatives we get the inequality

$$|d_{\Delta_i}| \leq e^{-t} C_3 + \int_0^t e^{-t} (K_6 e^{\tau/2} C + K_7 e^{\tau/2} + e^\tau K_5 |d_{\Delta_i}|) d\tau$$

where we can apply the Lemma of Gronwall. With $K_{12} := 2(K_6 C + K_7)$, $K_{13} := K_5 e^{K_5} C_3$ and $K_{14} := K_5 e^{K_5} K_{12} 2$ we get the bounds on $|d_{\Delta_i}(t)|$. From this we know that d_{Δ_i} can be written as

$$d_{\Delta_i}(t) = e^{-t}(\bar{d}_1(t) + t\bar{d}_2(t)) + \bar{d}_3(t)(e^{-t/2} - e^{-t})$$

with $|\bar{d}_1(t)| \leq C_3$, $|\bar{d}_2(t)| \leq K_{13}$, $|\bar{d}_3(t)| \leq K_{14}$. We use these relations in the equation for h_{Δ_i} and get

$$\begin{aligned} h_{\Delta_i} &= h_{i\Delta_i} + \int_0^t \tilde{H}_{\Delta_i} d\tau \\ &= h_{i\Delta_i} + \int_0^t (\tilde{H}_d d_{\Delta_i} + \tilde{H}_h h_{\Delta_i} + \tilde{H}_\Delta e^{-\tau/2}) d\tau. \end{aligned}$$

Taking the absolute value and using the bounds of the terms in the equation leads to

$$|h_{\Delta_i}| \leq r_i C_4 + \int_0^t (C_1 r_i (e^{-\tau/2} C_3 + K_{13}\tau e^{-\tau/2} + K_{14}(1 - e^{-\tau/2})) + C_2 r_i + K_9 r_i |h|_{\Delta_i}) d\tau,$$

where we can apply the Lemma of Gronwall again. If $C_5 := C_1(C_3 2 + K_{13}4)$ and because there exists a $C_6 \geq C_2 + r_i t C_5 + r_i t^2/2 C_2$ for $t \in [0, T]$ we get the bounds on $|h_{\Delta_i}|$. We see that for r_i sufficiently small, $T = 2ln(\rho/r_i)$ the assumption $|h_{\Delta_i}(t)| \leq r_1 C_5 + C_6 r_i T < C$ is satisfied (analogously to Lemma 17). □

For the derivatives with respect to r_i we get a similar result:

Proposition 9. *With $|d_i(r_i, \Delta_i)_{r_i}| \leq C_7$ and $|h_i(r_i, \Delta_i)_{r_i}| \leq C_8$ the derivatives satisfy*

$$|d_{r_i}(t)| \leq e^{-t} C_7 + K_{16} r_i^{-\alpha} e^{-t/2} + K_{17}$$
$$|h_{r_i}(t)| \leq C_{10} + K_{18} t$$

for some small constants K_{16}, K_{17}, K_{20} and constants C_7, C_{10}.

Proof: The proof is analogous to the previous Theorem. Especially we get the equations

$$|d_{r_i}| \leq e^{-t} C_7 + \int_0^t e^{-t+\tau} (K_6 e^{\tau/2} C r_i^{\alpha} + K_8 + K_5 |d_{r_i}|) d\tau$$

and

$$|h_{r_i}| \leq C_8 + \int_0^t (K_{18} + K_{19} r_i e^{-\tau/2} + K_9 r_i |h|_{r_i}) d\tau.$$

With new constants $K_{15} := K_6 C2$, $K_{16} := K_{15} + K_5 e^{K_5} K_{15} 2$, $K_{17} := K_8 + K_5 e^{K_5}(C_7 + K_8)$, $C_9 := C_8 + C_1 \rho 2 C_7$, $K_{19} := C_1 K_{16}$ and because there exists a constant $C_{10} \geq C_9 + r_1^{1-\alpha} K_{19} + K_9 e^{K_9 \rho} r_i (C_9 t + K_{18} t^2/2 + r_i K_{19} t^2/2)$ for $t \in [0, T]$, we get the statement of the Proposition. Again we see that for r_i sufficient small and $T = ln(\rho/r_i)$, the assumption $|r_i^{\alpha} h_{r_i}(t)| \leq r_i^{\alpha}(C_{10} + K_{18} T) < C$ is satisfied. □

Because T only depends on r_i, and

$$\frac{\partial}{\partial \Delta_i}(d(T)) = d_{\Delta_i}(T), \ \frac{\partial}{\partial \Delta_i}(h(T)) = h_{\Delta_i}(T),$$

$$\frac{\partial}{\partial r_i}(d(T)) = d_{r_i}(T) + d'(T) T_{r_i}, \ \frac{\partial}{\partial r_i}(h(T)) = h_{r_i}(T) + h'(T) T_{r_i}$$

we obtain Proposition 4.

This paper is based on results obtained in the Ph.D.-Thesis [11] of the first author under the guidance of the second author.

REFERENCES

[1] E. Arimodo, P. Bootz, P. Glorieux and E. Menchi, *Pulse shape and phase diagram in the passive Q switching of CO_2lasers,* J. Opt. Soc. Amer. B 2 (1985), pp. 193-201

[2] T. Carr, T. Erneux, *Dimensionless Rate Equations and Simple Conditions for Self-Pulsing in Laser Diodes,* IEEE J. Quant. Electr. 37 (2001), pp.1171-1177

[3] S-N. Chow, C. Li and D. Wang, *Normal Forms and Bifurcation of Planar Vector Fields,* Cambridge University Press, Cambridge, 1994

[4] F. Dumortier, *Techniques in the Theory of Local Bifurcations: Blow up, Normal Forms, Nilpotent Bifurcations, Singular Perturbations*; in Bifurcations and Periodic Orbits of Vector Fields, 1993, pp. 19-73

[5] F. Dumortier, R.Roussarie, *Canard Cycles and Center Manifolds,* Memoires of the AMS 557 (1996)

[6] F. Dumortier, R. Roussarie, *Multiple canard cycles in generalized Lienard equations*, J.Diff.Equ. 174 (2001), pp. 1-29
[7] T. Erneux, *Q-Switching Bifurcation in a Laser with a Saturable Absorber*, J. Opt. Soc. Amer. B 5 (1988), pp. 1063-1069
[8] T. Erneux, *Multiple time scale analysis of lasers*, in Fundamental Issues of Nonlinear Laser Dynamics, AIP Conference Proceedings 548 (2000), pp. 54-65
[9] T. Erneux, A. Gavrielides, P. Peterson, M. P. Sharma, *Dynamics of passively Q-switched microchip lasers*, IEEE J. Quant. Elect. 35 (1999), pp. 1247-1256
[10] T. Erneux, A. Gavrielides, P. Peterson, *The Pulse Shape of a Passively Q-Switched Microchip Laser*, Eur. Phys. J. D 10 (2000), pp. 423-431
[11] A. Huber, *Singularly Perturbed Laser Equations – Slow-Fast Dynamics of the Yamada Model*, PhD-Thesis, Vienna University of Technology, 2002
[12] H. Kawaguchi, *Bistabilities and nonlinearities in laser diodes*, Artech House, Boston (1994)
[13] G. Kozyreff, T. Erneux, *Singular Hopf bifurcation to strongly pulsating oscillations in lasers containing a saturable absorber*, Eur. J. Appl. Math. 14 (2003), pp. 407-420
[14] J. Dubbeldam, B. Krauskopf, *Self-pulsation of lasers with saturable absorber: dynamics and bifurcations*, Opt. Commun. 159 (1999), pp. 325-338
[15] J. Dubbeldam, B. Krauskopf, D. Lenstra, *Excitability and coherence resonance in lasers with saturable absorber*, Phys. Rev. E 60 (1999), pp. 6580-6588
[16] N. Fenichel, *Geometric Singular Perturbation Theory*, J.Diff.Equ. 31 (1979), pp.53-98
[17] J. Guckenheimer, P. Holmes, *Nonlinear Oscillations, Dynamical Systems, and Bifurcations of Vector Fields*, Springer, New York 1983
[18] C.K.R.T. Jones, *Geometric singular perturbation theory*, in Dynamical Systems, Springer Lecture Notes Math. 1609 (1995), pp. 44-120
[19] C. Jones, T. Kaper, *A primer on the exchange lemma for fast-slow systems*, in Multiple-Time-Scale Dynamical Systems, IMA volumes in mathematics and its applications 122 (2001), pp. 65-87
[20] B. Krauskopf, D. Lenstra, *Fundamental Issues of Nonlinear Laser Dynamics*, AIP Conference Proceedings 548, Melville, New York, 2000
[21] G. J. Spühler, R. Paschotta, R. Fluck. B. Braun, M. Moser, G. Zhang, E. Gini and U. Keller, *Experimentally confirmed design guidelines for passively Q-switched microchip lasers using semiconductor saturable absorbers*, J. Opt. Soc. Amer. B 16 (1999), pp. 376-388
[22] M. Krupa, P. Szmolyan, *Extending geometric singular perturbation theory to non-hyperbolic points - fold and canard points in two dimensions*, SIAM J. Math. Anal. 33 (2001), pp. 286-314
[23] M. Krupa, P. Szmolyan, *Extending Slow Manifolds near Transcritical and Pitchfork Singularities*, Nonlinearity 14 (2001), pp. 1473-1491
[24] M. Tachikawa, K. Tanii and T. Shimizu, *Comprehensive interpretation of passive Q switching and optical bistability in a CO_2 laser with an intracavity saturable absorber*, J. Opt. Soc. Amer. B 4 (1987), pp. 387-395
[25] F. Takens, *Partially hyperbolic fixed points*, Topology 10 (1971), pp. 133-147
[26] W. Walter, *Differential and integral inequalities*, Springer-Verlag, New York, 1970
[27] C. Weiss, R. Vilaseca, *Dynamics of Lasers*, VCH Publishers, Weinheim, 1991
[28] M. Yamada, *A theoretical analysis of self-sustained pulsation phenomena in narrow-stripe semiconductor lasers*, IEEE J. Quant. Elect. 29 (1993), pp. 1330-1336
[29] J. J. Zayhowski, *Ultraviolet generation with passively Q-switched microchip lasers*, Opt. Lett. 21 (1996), pp 588-590